

Non-Nucleoside Inhibitors of Human Adenosine Kinase: Synthesis, Molecular Modeling, and Biological Studies

Stefania Butini,^{†,‡} Sandra Gemma,^{†,‡} Margherita Brindisi,^{†,‡} Giuseppe Borrelli,^{†,‡} Andrea Lossani,^{†,§} Anna Maria Ponte,^{†,§} Andrea Torti,^{†,§} Giovanni Maga,^{†,§} Luciana Marinelli,^{†,‡} Valeria La Pietra,^{†,‡} Isabella Fiorini,^{†,‡} Stefania Lamponi,^{†,‡} Giuseppe Campiani,^{*,†,‡} Daniela M. Zisterer,^{||} Seema-Maria Nathwani,^{||} Stefania Sartini,[⊥] Concettina La Motta,[⊥] Federico Da Settimo,[⊥] Ettore Novellino,^{†,‡} and Federico Focher^{†,§}

[†]European Research Centre for Drug Discovery and Development (NatSynDrugs), Università di Siena, 53100 Siena, Italy

[‡]Dipartimento Farmaco Chimico Tecnologico, Via Aldo Moro, Università di Siena, 53100 Siena, Italy

[§]Istituto di Genetica Molecolare, CNR, Via Abbategrosso 207, 27100 Pavia, Italy

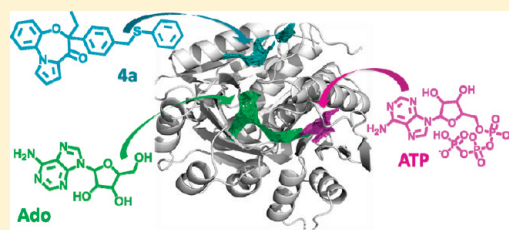
^{||}School of Biochemistry and Immunology, Trinity College, Dublin 2, Ireland

[⊥]Dipartimento di Scienze Farmaceutiche, Università di Pisa, Via Bonanno, 6, 56126 Pisa, Italy

^{*}Dipartimento di Chimica Farmaceutica e Tossicologica, Università di Napoli Federico II, Via D. Montesano 49, 80131 Napoli, Italy

S Supporting Information

ABSTRACT: Adenosine kinase (AK) catalyzes the phosphorylation of adenosine (Ado) to AMP by means of a kinetic mechanism in which the two substrates Ado and ATP bind the enzyme in a binary and/or ternary complex, with distinct protein conformations. Most of the described inhibitors have Ado-like structural motifs and are nonselective, and some of them (e.g., the tubercidine-like ligands) are characterized by a toxic profile. We have cloned and expressed human AK (*hAK*) and searched for novel non-substrate-like inhibitors. Our efforts to widen the structural diversity of AK inhibitors led to the identification of novel non-nucleoside, noncompetitive allosteric modulators characterized by a unique molecular scaffold. Among the pyrrolobenzoxa(thia)zepinones (**4a–qq**) developed, **4a** was identified as a non-nucleoside prototype *hAK* inhibitor. **4a** has proapoptotic efficacy, slight inhibition of short-term RNA synthesis, and cytostatic activity on tumor cell lines while showing low cytotoxicity and no significant adverse effects on short-term DNA synthesis in cells.



INTRODUCTION

Adenosine kinase (AK, EC 2.7.1.20) is a ubiquitous intracellular purine metabolic enzyme that plays a key role in the control of intra- and extracellular concentration of adenosine (Ado, **1**, Chart 1). Once inside the cell, Ado is rapidly phosphorylated to Ado monophosphate (AMP) by AK, using the γ -phosphate of the second substrate Mg/ATP^{2–}. This maintains low intra- and extracellular concentrations of Ado, since Ado uptake is driven by its concentration gradient. While at low substrate concentrations the phosphorylation reaction follows Michaelis–Menten kinetics, Ado phosphorylation is subjected to uncompetitive substrate (Ado) inhibition.¹ This could probably be explained by hypothesizing that Ado binds not only the catalytic site but also a regulatory site with lower affinity, being responsible for phosphorylation rate modulation.^{2–5}

Ado has been characterized as a homeostatic modulator of cellular activity and has several important roles in central and peripheral nervous systems (CNS, PNS), where the fine-tuning of its concentrations holds a particular physiological relevance.^{6,7} The multitude of Ado effects are mediated by the activation of specific metabotropic receptors; four receptor subtypes have

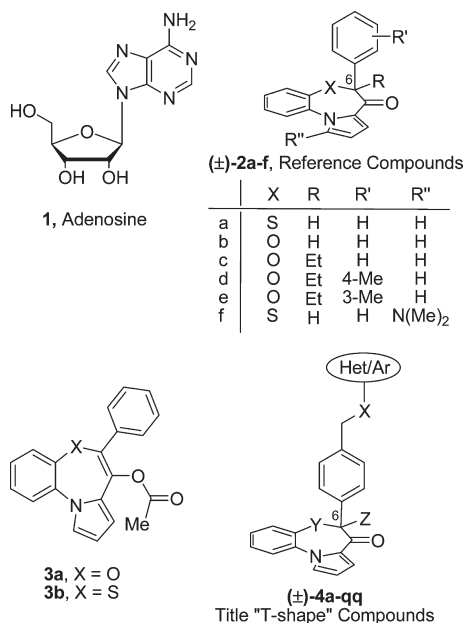
been identified and cloned (A₁, A_{2A}, A_{2B}, and A₃) to date.⁸ Ado behaves as an endogenously released neuromodulator of intercellular signaling that reduces cell excitability during tissue stress and trauma.^{8,9} In fact, it has been observed that the local Ado concentration increases at sites of inflammation or tissue damage.¹⁰ Ado exerts its antinociceptive and anti-inflammatory effects by functioning as a negative feedback signal whose responses tend to decrease cellular activity, increase local nutrient supply, and restore normal cellular functions.¹¹ Moreover, Ado plays a neuroprotective role during ischemic episodes and acts as an anticonvulsant in spontaneous or induced seizures in animals or epileptic patients.^{11,12}

Emerging evidence has focused upon the role of Ado on cell death and differentiation. Extracellular Ado induces apoptosis in human epithelial cancer cells originating from breast, colon, and ovary via the intrinsic or mitochondrial pathway.^{13–15} Ado uptake into cells through Ado transporters and its ensuing conversion to AMP by AK increase the intracellular AMP concentration, thus triggering the AMP-activated protein kinase.

Received: November 9, 2010

Published: February 14, 2011

Chart 1. Reference and Tile Compounds



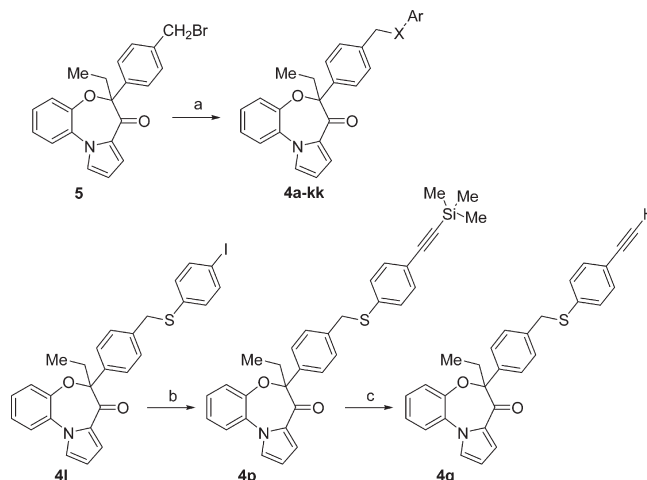
Ado-induced cell death (apoptosis) may occur via both receptor-mediated and non-receptor-mediated pathways.

Selective human AK (*hAK*) inhibitors may potentiate extracellular Ado levels, enhancing the endogenous protective effect of Ado.¹¹ Accordingly, AK inhibitors have been shown to provide antinociceptive, anti-inflammatory, and anticonvulsant activity in animal models, thus suggesting their potential therapeutic utility for pain, inflammation, epilepsy, and possibly other CNS and PNS diseases associated with cellular trauma and inflammation.^{16,17}

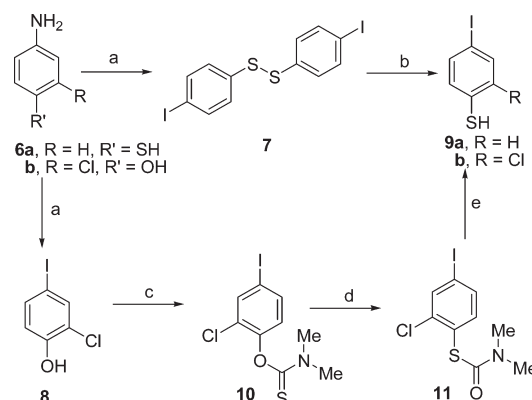
The reports of Ado-induced apoptosis have suggested a potential role for AK inhibitors in cancer therapy.¹⁸ However, the direct involvement of Ado in apoptosis is still controversial. In fact, while some AK inhibitors described by Mlejnek and co-workers¹⁹ prevented cells from going into apoptosis, other authors demonstrated that Ado induces apoptosis in human leukemia (HL-60) cells.²⁰

In recent years we have attempted to develop novel proapoptotic agents, interfering with tubulin or mitochondrial permeability proteins and blocking the cell cycle in the G₁ or G₂/M phase.²¹ Consequently, we selected the *hAK* as an interesting target to develop novel potential proapoptotic agents. Potent AK modulators have been recently described, most of them competitively binding the Ado binding site and containing Ado-like structural motifs.²² In order to reduce the nucleotide structural similarities and to optimize the biological properties, recently a systematic approach has been taken to dismantle the nucleoside structure of the early inhibitors, from tubercidine-like compounds to pyridopyrimidines and later to alkynylpyrimidines.¹⁶

To identify novel non-nucleoside *hAK* inhibitors (NN*hAK*Is), a biological screening of our in house database of proprietary compounds was performed. Compounds 2a–f and 3a,b (Chart 1) were identified as interesting molecular hits that were taken as starting points for structure–activity relationship (SAR) studies through the synthesis of derivatives 4a–qq. Our efforts to widen the structural diversity of *hAK* inhibitors so far reported^{16,22,23} led to the identification of novel noncompetitive modulators of the human enzyme,

Scheme 1. General Synthesis of Compounds 4a–kk^a

^a Reagents and conditions: (a) (Het)ArSH or ArOH, NaH 60% in mineral oil, dry THF, room temp, 9 h; (b) PdCl₂(PPh₃)₂, CuI, trimethylsilylacetylene, triethylamine (TEA), room temp, 9 h; (c) K₂CO₃, MeOH, THF, room temp, 45 min.

Scheme 2. Synthesis of Iodo(thio)phenol Intermediates^a

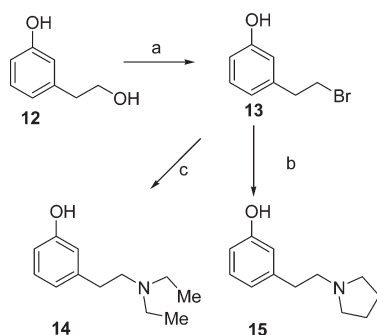
^a Reagents and conditions: (a) NaNO₂, KI, urea, HCl, H₂SO₄, H₂O, 0 °C, 5 h; (b) NaBH₄, MeOH, 3 h; (c) DABCO, Me₂NC(S)Cl, dimethylformamide (DMF), room temp, 1 h; (d) microwave, 220 °C, 150 W, 10 min; (e) 3 N KOH, EtOH, 3 h.

characterized by a molecular scaffold not reminiscent of the substrate Ado.

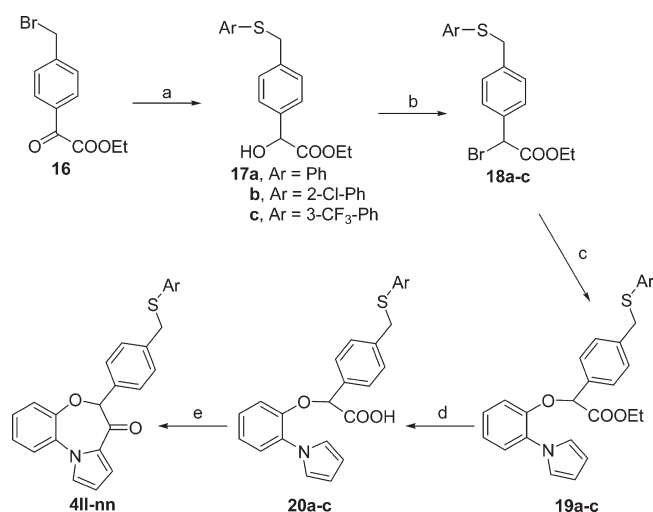
CHEMISTRY

The synthesis of compounds 4a–qq is reported in Schemes 1–5. As outlined in Scheme 1, for the synthesis of compounds 4a–kk (Chart 1 and Tables 2 and 3) the bromo derivative 5²⁴ was used as the alkylating agent of the appropriate (hetero)arylthiophenols and phenols previously deprotonated with sodium hydride. Starting from 4l, application of the Sonogashira protocol furnished compound 4p from which, after treatment with potassium carbonate in MeOH and tetrahydrofuran (THF), compound 4q was obtained.

The noncommercially available thiols and phenols were synthesized as reported in Schemes 2 and 3. The iodobenzenethiols needed for the synthesis of compounds 4l and 4bb were obtained starting from 4-aminobenzenethiol 6a or from 4-amino-2-chlorophenol 6b. Compounds 6a,b were subjected to a

Scheme 3. Synthesis of Substituted Phenol Intermediates^a

^a Reagents and conditions: (a) CBr₄, PPh₃, dry MeCN, reflux, 12 h; (b) diethylamine, TEA, dry MeCN, reflux, 12 h; (c) pyrrolidine, TEA, dry MeCN, reflux, 12 h.

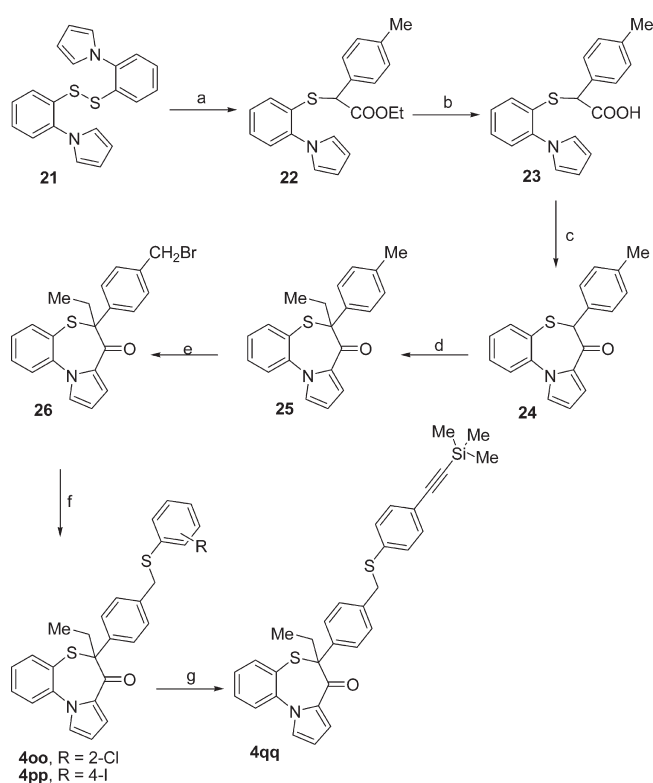
Scheme 4. Synthesis of Compounds 4ll–nn^a

^a Reagents and conditions: (a) Ar-S-S-Ar/Ar-SH, NaBH₄, NaH, dry THF, 25–60 °C, 12 h; (b) PPh₃, CBr₄, MeCN, 50 °C, 12 h; (c) 2-(pyrrol-1-yl)phenol, NaH, dry THF, 40 °C, 11 h; (d) NaOH, THF/EtOH 1:1, room temp, 12 h; (e) PCl₅, dry dichloromethane (DCM), reflux, 7 h.

Sandmeyer reaction to give the corresponding iodo derivatives 7 and 8 (Scheme 2). Sodium borohydride reduction of the disulfide 7 furnished the 4-iodobenzenethiol 9a. The synthesis of the S-aryl thiocarbamate 11 was performed by formation of the O-aryl dimethylthiocarbamate 10 using dimethylthiocarbamyl chloride in the presence of 1,4-diazabicyclo[2.2.2]octane (DABCO).²⁵ The Newman–Kwart rearrangement (11) was conveniently performed under microwave irradiation. Finally, compound 11 was treated with potassium hydroxide to afford 2-chloro-4-iodobenzenethiol 9b.

The *m*-ethylphenol derivatives (14 and 15) used for the synthesis of compounds 4jj,kk were prepared starting from 3-(2-hydroxyethyl)phenol 12 (Scheme 3). Compound 12 was brominated in the presence of carbon tetrabromide and triphenylphosphine in acetonitrile. The obtained bromo derivative 13 was used as the alkylating agent for diethylamine and pyrrolidine to give the phenols 14 and 15, respectively.

Compounds 4ll–nn were synthesized as described in Scheme 4. The bromo derivative ethyl 2-[4-(bromomethyl)phenyl]-2-oxoacetate 16²⁶ was the alkylating agent for the

Scheme 5. Synthesis of Compounds 4oo–qq^a

^a Reagents and conditions: (a) (±)-α-bromo-*p*-tolylacetic acid ethyl ester, NaBH₄, absolute EtOH, reflux, 8 h; (b) NaOH, THF/EtOH, room temp, 12 h; (c) PCl₅, dry DCM, reflux, 12 h; (d) ethyl iodide, KH 30% in mineral oil, dry THF, room temp, 15 h; (e) *N*-bromosuccinimide, 2,2'-azodiisobutyronitrile (AIBN), CCl₄, reflux, 2.5 h; (f) ArSH, NaH 60% in mineral oil, dry THF, room temp, 12 h; (g) from 4pp, PdCl₂(PPh₃)₂, CuI, trimethylsilylacetylene, TEA, room temp, 9 h.

appropriate thiophenols, and the resulting intermediates were immediately reduced with sodium borohydride. The racemic secondary alcohols 17a–c were brominated with carbon tetrabromide/triphenylphosphine, and the bromides (18a–c) were used to alkylate the 2-(pyrrol-1-yl)phenol.²⁴ The esters 19a–c were then hydrolyzed to the corresponding acids 20a–c which underwent an intramolecular Friedel–Crafts cyclization giving the final compounds (4ll–nn) as racemic mixtures.

The synthesis of compounds 4oo–qq is reported in Scheme 5. The reduction–alkylation reaction of 21²⁷ with the ethyl ester of (±)-α-bromo-*p*-tolylacetic acid in the presence of sodium borohydride afforded the intermediate 22. After saponification of the ester 22, the acid 23 was cyclized (24) as previously described. The cyclic ketone 24 was C-6 alkylated (25) and brominated (26) by means of a radicalic bromination. Compounds 4oo and 4pp were obtained by reaction of the bromo derivative 26 with 2-chlorobenzenethiol and 4-iodobenzenethiol (9a), respectively, in the presence of sodium hydride. Finally, application of Sonogashira protocol with trimethylsilylacetylene on compound 4pp afforded compound 4qq.

RESULTS AND DISCUSSION

Cloning, Expression, and Biochemical Characterization of hAK. Messenger RNA for hAK was identified in GenBank (accession number BC003568). Amplified cDNA was obtained

by using RT-PCR applied on total HeLaS-3 RNA with sense and antisense primers as reported in the Experimental Section. The amplified region, containing the complete *hAK* coding sequence, was inserted into the multiple cloning site of pTrcHisA (Invitrogen) to give the recombinant bacterial expression vector pHis-*hAK*. His-tagged *hAK* sequence encodes for the complete 345 amino acids enzyme with a 6-His tag at its NH₂ terminus.

Expression and purification of *hAK* was carried out as described in Experimental Section. The enzyme was purified from *E. coli* crude extract in a single chromatographic step by using a Ni-NTA Superflow column. Recombinant *hAK* had a specific activity of 38 500 units/mg (1 unit is defined as the amount of enzyme catalyzing the formation of 1 nmol of AMP in 1 h at 37 °C). Figure 1 of the Supporting Information shows the SDS-PAGE of the purification of recombinant *hAK* (MW = 46 kDa).

In order to determine the kinetic parameters of recombinant *hAK*, we incubated the enzyme in the presence of different concentration of substrate (Ado) using ATP as phosphate donor at 1 mM. Table 1 reports the experimental kinetic parameters of the enzyme. In a substrate concentration range between 0.1 and 2 μ M, recombinant *hAK* phosphorylates Ado following typical Michaelis-Menten kinetics ($K_m = 0.4 \mu$ M).

Inhibition Assays on the Recombinant *hAK*. Following our previous experience with the synthesis of non-nucleoside inhibitors of HIV-1 reverse transcriptase^{24,28–30} and hepatitis C virus nonstructural protein 3 enzyme,³¹ in order to identify novel *hAK* non-nucleoside inhibitor hits, we screened various classes of polycyclic compounds that include quinolines, pyrroloquinoxalines, benzazepinones, benzodiazepinones, pyrrolobenzothiazepinones, pyrrolobenzoxazepines, dibenzazepines, and dibenzothiazepines, all available in our laboratories. Among the tested compounds we found that pyrrolobenzoxa(thia)zepinones showed an inhibitory activity in the high micromolar range (**2a–f**, Chart 1), indicating such scaffolds as suitable for the development of specific NN*hAK*Is (Chart 1). Thus, the objective of this study was the development of a novel class of noncompetitive NN*hAK*Is with the pyrrolobenzoxa(thia)zepinone core and drawing of SARs for *hAK* inhibition related to the variation of the substituents on the heterocyclic system. The *hAK* inhibition potency of prototypic compounds is reported in Table 2.

Compounds **2a–e** are the representative of a class of non-nucleoside inhibitors of HIV-1 reverse transcriptase.^{24,30} The benzothiazepine **2a** proved to be less potent than the corresponding C-6 monosubstituted benzoxazepine (**2b**) and benzoxazepines bearing an alkyl chain (R) at C-6 (**2c,d**), probably because of the different geometry of the polycyclic system. A methyl group at the para position on the phenyl at C-6 was better tolerated than at the meta position (**2d** vs **2e**). The insertion of a substituent (R'') on the pyrrole ring led to compound **2f**³² that displayed no activity at 10^{−3} M. The critical role of the geometry of the system (and possibly also the addition of bulky groups at C-5) was also confirmed by the lack of activity of esters **3a,b**,³³ presenting a planar and conjugated pyrrolobenzoxa(thia)zepine system.

On the basis of the results obtained and with the aim to improve enzyme inhibitory potency, we synthesized compounds **4a–qq** (Chart 1) presenting a pyrrolo[2,1-*d*]benzoxa(thia)zepinone scaffold with a “T-shape” geometry and bearing a variety of substituents at C-6 (Tables 3 and 4), so maintaining the core system and geometry of compounds **2**.

The SAR studies were widely explored with respect to the introduction of substituted (hetero)arylthiomethyl and phenoxymethyl functions at the para position of the C-6 pendant phenyl

Table 1. Kinetic Parameters of Recombinant *hAK* with ATP as Phosphate Donor

substrate	K_m (μ M)	V_{max} ($\text{pmol s}^{-1} \mu\text{g}^{-1}$)	k_{cat}^a (s^{-1})	k_{cat}/K_m^a ($\text{s}^{-1} \mu\text{M}^{-1}$)
adenosine	0.4 ± 0.1	10.7 ± 1.0	0.5	1.25

^a k_{cat} was calculated by using 46.0 kDa as the molecular mass of the enzyme.

Table 2. IC₅₀ (μ M) on *hAK* for Reference Compounds

Compd	Structure	<i>hAK</i> (IC ₅₀) ^a
(±)- 2a		130
(±)- 2b		100
(±)- 2c		85
(±)- 2d		80
(±)- 2e		150
(±)- 2f		>1000
(±)- 3a		NA
(±)- 3b		NA

^a Each value is the mean of at least three determinations. Standard error of the mean (SEM) is $\leq 10\%$.

ring of both the pyrrolobenzoxazepinone and pyrrolobenzothiazepinone scaffolds. The effect of removal of the C-6 ethyl group was also evaluated. All the compounds were tested as racemates, but to evaluate a possible stereoselective mechanism of enzyme inhibition, the racemic mixture of derivative **4s** was resolved by HPLC techniques into the pure (+)- and (–)-enantiomers, which were tested in the enzyme inhibition assays.

All the explored modifications of the structures of 6-ethyl-6-phenylpyrrolobenzoxazepinones are grouped into the following subsets of inhibitors: (i) arylmercaptomethyl derivatives (**4a–cc**, Table 3), (ii) heteroarylmercaptomethyl derivatives (**4dd–gg**, Table 4), (iii) phenoxy derivatives (**4hh–kk**, Table 4), (iv) C-6-desethyl analogues (**4ll–nn**, Table 4), and (v) thiazepinone analogues (**4oo–qq**, Table 4).

i. Arylmercaptomethyl Derivatives. A large series of 6-ethyl-6-arylpyrrolobenzoxazepinones (**4a–cc**, Table 3) bearing substituted arylmercaptomethyl groups at the C-6 phenyl moiety in para position was synthesized and tested. The effects of mono-, di-, tri-, and tetrasubstitutions with electron-withdrawing groups (EWGs) or electron-donating groups (EDGs) were evaluated.

SARs analysis of the inhibition data obtained with the mono-substituted compounds demonstrated that with respect to the unsubstituted derivative **4a** ($IC_{50} = 1.2 \mu M$), ortho substitution with halogens is well tolerated (**4a** vs **4b,c**). Similarly, the meta position benefits of EWGs (compounds **4e–g,i** displayed IC_{50} between 2.5 and 4.0 μM) rather than EDGs (**4d,h**). At the para position, halogen substitution was associated with better potency, following the trend $F > Br > I$ (**4j–l**). Other EWGs ($-NO_2$ and $-OCF_3$, **4m,n**) slightly lowered inhibition potency. In line with previous data, the presence of EDGs (such as the methoxy and the alkyne, **4o–q**) lowered potency by one order of magnitude (**4j** vs **4o–q**).

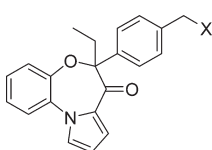
The arylmercaptomethyl moiety was also disubstituted leading to compounds **4r–bb**. In this subseries of analogues when the *o*-Cl functionality of **4c** was accompanied by an *o*-methyl group (**4r**), a compound 3 times less potent than **4c** was obtained. Disubstitution of the phenylmercapto moiety by halogens (**4t–z,bb,cc**) was generally tolerated, with **4bb** being the best performing with an IC_{50} of 2.0 μM . Interestingly, the inhibitory potency of **4bb** was similar to that of its corresponding aryloxy analogue **4hh** (Table 4), thus suggesting that bridging compounds with sulfur or oxygen does not interfere with potency. As expected, substitution of halogens by methoxy groups at C-2 and C-5 produced a weak inhibitor (**4aa**) of hAK.

Analysis of pure enantiomers (+)-**4s** and (–)-**4s** assays indicated a stereoselective interaction with the human enzyme, the (+)-enantiomer being about 5 times more potent than the corresponding (–)-enantiomer (Table 3).

ii. Heteroarylmercaptomethyl Derivatives. A subset of compounds was synthesized to evaluate the effect of substitution of the arylmercaptomethyl group by five/six membered nitrogen containing heterocycles (**4dd–gg**, Table 4). In general these compounds showed single digit inhibitory potencies, with the imidazole based analogue **4ee** being the most potent of the subseries (**4ee**, $IC_{50} = 3.5 \mu M$).

iii. Phenoxy methyl Analogues. A small series of C-6 phenoxy methylphenyl substituted derivatives (**4hh–kk**, Table 4) was synthesized. Notably the 2-chloro-4-iodophenoxy substituted analogue **4hh** was a potent hAK inhibitor ($IC_{50} = 1.2 \mu M$), almost 2-fold more potent than the sulfur bridged analogue **4bb**.

Table 3. IC_{50} (μM)^a on hAK for Compounds **4a–cc**



Compd	X	IC_{50}	Compd	X	IC_{50}
(±)- 4a		1.2	(±)- 4q		15.0
(±)- 4b		4.5	(±)- 4r		3.0
(±)- 4c		1.0	(±)- 4s		20.0
(±)- 4d		21.4	(–)- 4s		40.0
(±)- 4e		4.0	(+)- 4s		7.5
(±)- 4f		3.5	(±)- 4t		3.0
(±)- 4g		2.5	(±)- 4u		14.0
(±)- 4h		12.5	(±)- 4v		22.5
(±)- 4i		3.2	(±)- 4w		10.0
(±)- 4j		1.0	(±)- 4x		10.0
(±)- 4k		2.0	(±)- 4y		2.5
(±)- 4l		2.5	(±)- 4z		11.0
(±)- 4m		6.2	(±)- 4aa		35.0
(±)- 4n		6.7	(±)- 4bb		2.0
(±)- 4o		14.0	(±)- 4cc		8.0
(±)- 4p		10.0			

^a Each value is the mean of at least three determinations. SEM is $\leq 10\%$.

Table 4. IC_{50} (μM)^a on *hAK* for Compounds 4dd–qq and Calculated Single pK_a for Selected Compounds

Compd	X	Y	Z	IC_{50}	Single pK_a ^b
(±)-4dd		O	Et	4.5	N = 2.81
(±)-4ee		O	Et	3.5	N = 5.47 NH = 12.47
(±)-4ff		O	Et	7.0	N ₁ = -0.89 N ₄ = -0.16
(±)-4gg		O	Et	7.0	N ₁ = -0.18 N ₅ = -0.18
(±)-4hh		O	Et	1.2	
(±)-4ii		O	Et	8.0	
(±)-4jj		O	Et	200	N = 10.2
(±)-4kk		O	Et	150	N = 10.2
(±)-4ll		O	H	4.0	
(±)-4mm		O	H	4.4	
(±)-4nn		O	H	9.0	
(±)-4oo		S	Et	5.0	
(±)-4pp		S	Et	2.2	
(±)-4qq		S	Et	2.0	

^a Each value is the mean of at least three determinations. SEM is $\leq 10\%$.

^b Apparent pK_a values (ACD/Labs, version 12.0, Toronto Canada).

We also explored the tolerance of longer side chains, bringing or not protonatable groups (4ii and 4jj,kk). While the hydrophilic OH group of 4ii (IC_{50} = 8.0 μM) was still tolerated, the protonatable and bulkier lateral chains of 4jj,kk determined a dramatic drop of potency.

iv. C-6-Desethyl Derivatives. To establish the role of the ethyl chain at C-6, a series of C-6-desethyl analogues were synthesized

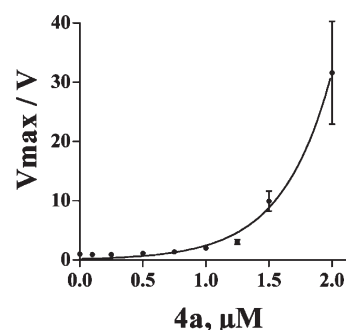


Figure 1. In vitro effect of increasing concentrations of 4a on *hAK* activity.

and tested (4ll–nn, Table 4). All compounds displayed a slightly lower inhibitory potency with respect to their ethyl-substituted counterparts (4ll vs 4a, 4mm vs 4c, and 4nn vs 4g) that could be either due to a different conformational preference for the tricyclic scaffold or due to the lack of favorable hydrophobic interaction of the ethyl chain with the enzyme.

v. Pyrrolobenzothiazepinone Derivatives. We also compared the potency of compounds based on a pyrrolo[2,1-*b*][1,4]benzoxazepinone skeleton with those based on a pyrrolo[2,1-*b*][1,4]benzothiazepinone tricyclic system (4oo–qq, Table 4), which again demonstrated that the replacement of the bridging oxygen was not essential for potency. Interestingly, in this subseries of compounds the introduction of an ethynylsilane moiety (4qq) in para position led to a compound more potent than the corresponding pyrrolobenzoxazepinone 4p.

Enzymatic Inhibition Kinetic Studies and Possible Site of Interaction within the *hAK*. Interestingly, the majority of compounds, tested as described in the Experimental Section, showed inhibitory activity on *hAK* in the micromolar range. The behavior of selected compounds 4a, 4e, and 4g (IC_{50} = 1.2, 4.0, and 2.5 μM , respectively) was studied more deeply. In general they showed hyperbolic curves of inhibition (Figure 1 for 4a) which indicate a nonlinear mode of action.

The inhibitory activity of 4a, representative of the whole series, was then evaluated in kinetic experiments with our cloned *hAK* in order to understand its site of binding and the mechanism of action.

It is known that two Ado binding sites exist on *hAK*, a catalytic site with high affinity for Ado and a low affinity regulatory site,⁵ probably partially overlapping the ATP binding site responsible for substrate inhibition by Ado.⁴

The *hAK* follows an obligatory ordered ternary complex reactant kinetic pathway for catalysis where the Ado binds first followed by ATP or Ado. Upon binding of the substrate Ado or upon binding of the second substrate ATP, a conformational rearrangement is observed. Indeed, native AK and AK complexed to Ado exist in a protein conformation distinct from AK complexed to Ado/ATP or to Ado/Ado (ternary complex).⁵ Thus, we can hypothesize that three different conformation/kinetic forms of the *hAK* exists with different affinities for specific ligands.

We tested the effect of 4a at different concentrations of both Ado and ATP. The inhibitory potency of 4a was unaffected by increasing concentrations of Ado (Figure 2) or ATP (data not shown), indicating a noncompetitive mode of inhibition.

Molecular Modeling. To rationalize the noncompetitive (Ado and ATP) mode of action combined with the micromolar

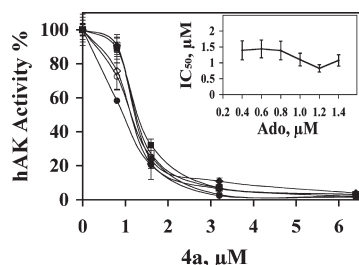


Figure 2. Effect of increasing concentrations of **4a** on *hAK* activity at different Ado concentrations: (◆), 0.4, (■) 0.6, (□) 0.8, (◇) 1.0, (●) 1.2, (○) 1.4 μM . Inner panel: IC_{50} , determined for each Ado concentration with Prism3 software through the formula $y = v/[1 + (x/\text{IC}_{50})]$, where v is the enzyme velocity and x is the **4a** concentration.

inhibitory activity found for the best modulators of the series, we hypothesized the existence of an allosteric site, whose accessibility may be dependent upon the conformational/kinetic state of the enzyme. However, to date there is no direct evidence of the existence of any allosteric site in *hAK*. So with the aim of identifying a binding site other than the catalytic/regulatory ones, the server Q-SiteFinder and the SiteMap software (Schrödinger) were both used either on a closed or on the open enzyme conformation. The closed structure 1BX4 (PDB code),⁵ cocrystallized with two Ado molecules and possessing the higher resolution, was selected together with the unique open structure available in the PDB (PDB code 2I6B)³⁴ which is complexed with a pyrimidin-4-ylamine analogue. The server Q-SiteFinder and the SiteMap software generated comparable results. Interestingly, in the closed enzyme conformation, beside the Ado and ATP binding sites, a shallow pocket, which is located between the helices $\alpha 3$, $\alpha 4$ and the long carboxylic tail and which is upon the Ado and ATP binding sites, was detected (see Figure 3). Intriguingly, such a site is just partially present in the open conformation of the enzyme because of the movement of the $\beta 4$ sheet. As nowadays it is well-known that in enzymes synergy between structure and plasticity results in the unique power of these biocatalysts, a ligand able to bind such a pocket would hamper the *hAK* conformational flexibility and in turn its catalytic activity, thus behaving as *hAK* inhibitor. Although the question of how enzymes achieve the catalytically competent state has recently become approachable by experimental and computational studies,³⁵ this is beyond the scope of this work. Herein, in order to verify the capability of **4a** to preferentially recognize the hypothesized allosteric site, a blind docking comprising the entire closed conformation of the enzyme was performed by means of the Autodock program. Amazingly, although the ligand can potentially bind other sites, in the lowest energy conformation family, **4a** was found to be well anchored in such a pocket (Figure 4). After the capability of **4a** to bind the putative allosteric site was probed, the Glide docking program was subsequently used to gain insights into the binding mode of **4a** at an atomic level (see Experimental Section for further details).

In the best scored binding pose (Figure 5), **4a** was found to bind the allosteric site with a well-defined “T-shape” geometry where the C-6 ethyl group lies between the T337 and the K71 residues and forms hydrophobic interactions with T and K side chains, while the benzene ring establishes a cation– π interaction with the K102 amine group (the distance between the aromatic ring centroid and the K nitrogen atom is 5.8 Å). An H-bond

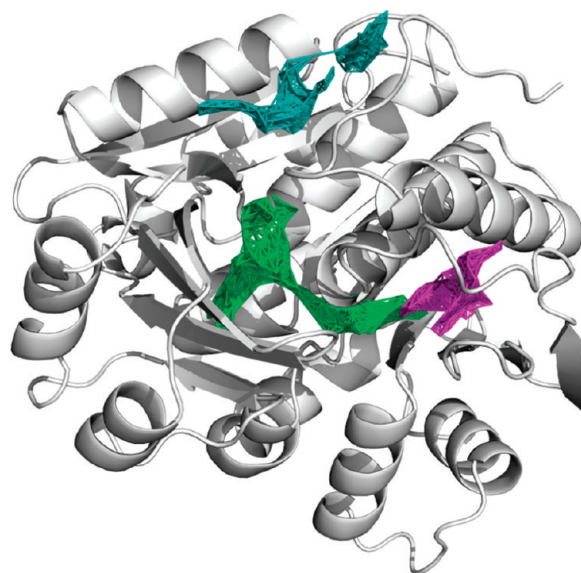


Figure 3. Putative allosteric site (cyan) in the close conformation of the *hAK* enzyme as identified by the Q-SiteFinder software. In the picture are also visible the Ado binding site (green) which extends toward the ATP binding site (violet).

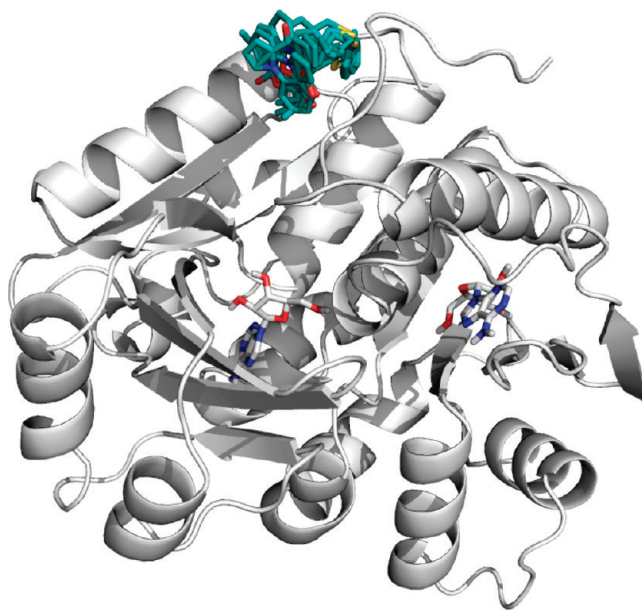


Figure 4. Lowest energy conformation family of **4a** resulting after the blind docking. **4a** can allocate in a site upon those of Ado, which are discernible because they contain the substrate molecule, shown as sticks.

between the carboxylic group of the oxazepinone ring and the backbone NH of F338 was also detected. On the other side of the molecule, the phenylmercaptomethyl group inserts into a well-defined pocket made up by Q74, Q79, H81, H107, and K341 and establishes a T-shaped interaction with H81. The above-described binding mode would be in line with the extensive SAR studies previously discussed. In fact compounds (**2a–e**) lacking the phenylmercaptomethyl moiety were all weaker *hAK* inhibitors than **4a**. Among them, **2b** is about 80-fold less potent than **4a**, as it lacks both the phenylmercaptomethyl moiety and the C-6 ethyl group. In line with the hydrophobic interactions

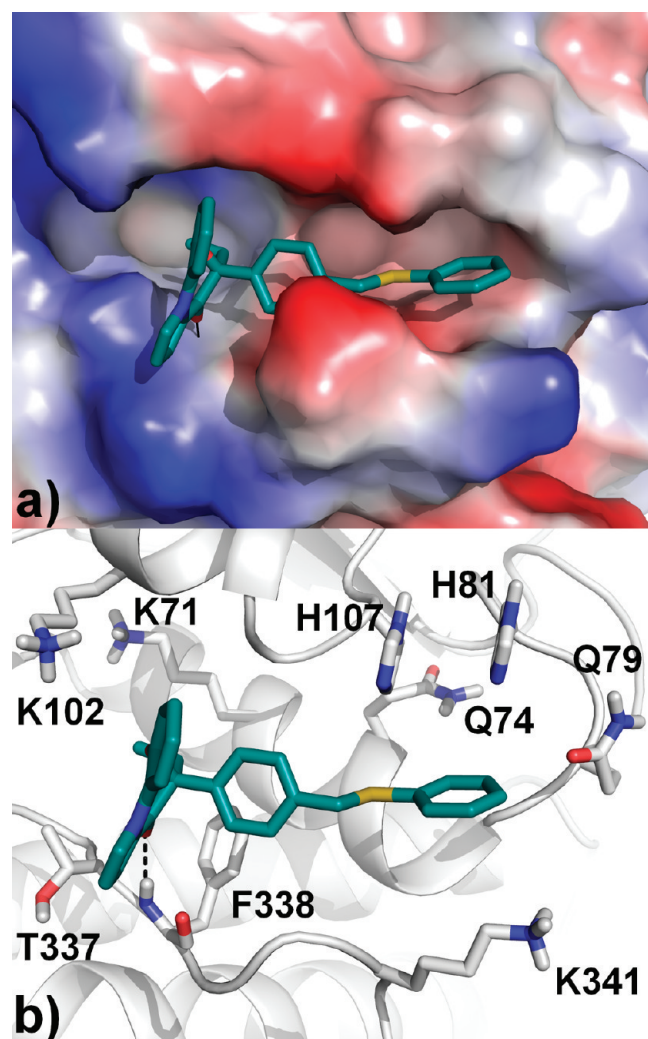


Figure 5. (a) Putative binding pose of **4a** in the allosteric site of hAK shown as surface and colored based on molecular electrostatic potential (MEP) as calculated by the PyMol program. (b) Putative binding pose of **4a** in the allosteric site of hAK shown as white cartoon. Interacting residues are shown as sticks and colored by atom type, while the H-bond is represented by a black dashed line.

formed by the ethyl group of **4a**, compounds **4ll–nn** are all less potent inhibitors than **4a**. In agreement with the importance of the “T-shape” geometry for a proper interaction with the enzyme site and in line with the limited space available for substitution on the oxazepinone ring, ligands **3a,b** are totally inactive. Taking into account the newly synthesized compounds **4a–cc** (Table 3), SARs indicated that the presence of EDGs, such as methyl (**4d**) or methoxy (**4h**), lowers the binding potency while the presence of EWG such as fluorine or chlorine atoms in ortho or meta position or iodine and bromine atoms in para position is well tolerated, and this would be in line with the T-shaped interaction established with H81 ring. Notably, insertion of other EWGs in para position, such as $-\text{NO}_2$ and $-\text{OCF}_3$ (**4m,n**), slightly lowered inhibition potency probably because of a major steric hindrance of these groups with respect to the other above-mentioned EWG. Docking experiments suggest that in **4d** and/or **4h** the lowered activity would not be due to a steric factor but to the presence of an EDG such as a methyl and a methoxy, which would disfavor the interaction of benzene with H81 electron-rich imidazole ring. Accordingly, a slight loss in

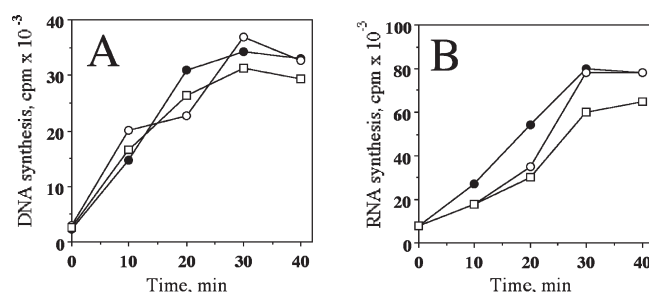


Figure 6. Effect of **4a** on short-term DNA (A) and RNA (B) syntheses in cell culture (HeLaS-3). Nucleic acids and protein syntheses were determined by measuring the incorporation of [^3H]thymidine and [^3H]uridine, respectively, in acid precipitable materials following the method described in Experimental Section: (●) 0 μM , (○) 10 μM , and (□) 50 μM **4a**. Each value is the mean of three determinations. SEM is $\leq 10\%$.

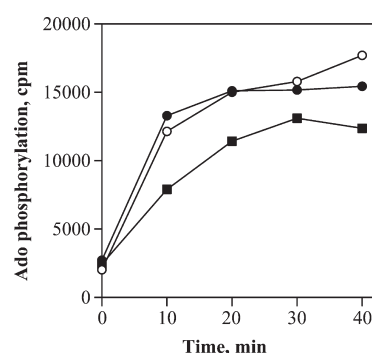


Figure 7. Effect of **4a** on HeLaS-3 cell Ado phosphorylation in vivo. For experimental details see Experimental Section: (●) 0 μM , (○) 2.5 μM , and (■) 25 μM **4a**. Each value is the mean of three determinations. SEM is $\leq 10\%$.

potency is also detectable for nitrogen containing electron-rich heterocycles (**4dd–gg**, Table 4). Finally, docking studies on compounds **4jj** and **4kk** suggest that the insertion in the phenyloxomethyl meta position of a N-protonated side chain would be not fruitful because of the narrow end of the pocket and the proximity of K341 protonated side chain. Thus, the binding mode of **4a** suggested by the Glide docking program is in line with the experimentally determined SARs and on one hand would sustain our hypothesis and on the other hand would validate the proposed binding pose. However, further experiments such as site-directed mutagenesis studies should be performed in the future to ultimately validate our assumptions.

In order to better characterize this class of non-nucleoside noncompetitive inhibitors of hAK, we selected **4a** as the reference compound for further biological studies.

Effect of 4a on in Vitro Short-Term DNA and RNA Syntheses and Cell Viability. In order to verify whether **4a** shows any effect in vitro on short time DNA and RNA syntheses, we incubated HeLaS-3 cells in the presence of 10 and 50 μM **4a** as described in the Experimental Section. In our assay conditions, as reported in Figure 6, **4a** does not significantly affect DNA synthesis but slightly interferes with RNA synthesis ($\text{IC}_{50} = 50 \mu\text{M}$).

In order to verify cellular permeability of compound **4a**, HeLaS-3 cells were incubated with the tested compound and its ability to inhibit in vitro phosphorylation of Ado was evaluated as described in the Experimental Section. The amount of produced [^3H]AMP was measured after co-incubation with different concentrations of **4a** at different times (Figure 7). This experiment indicates that after

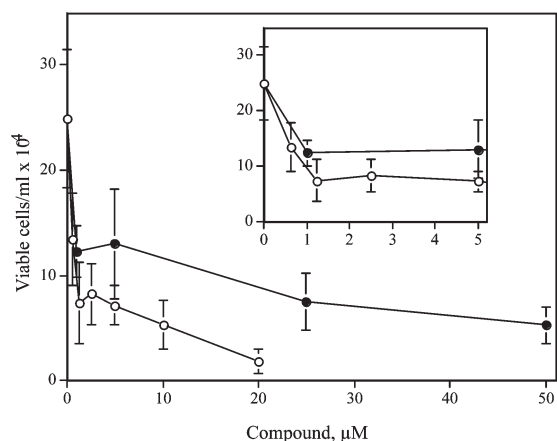


Figure 8. Effect of different concentrations of **4a** (●), and ddCyd (○) as control, on K562 cell line after 7 days of exposure to the compounds.

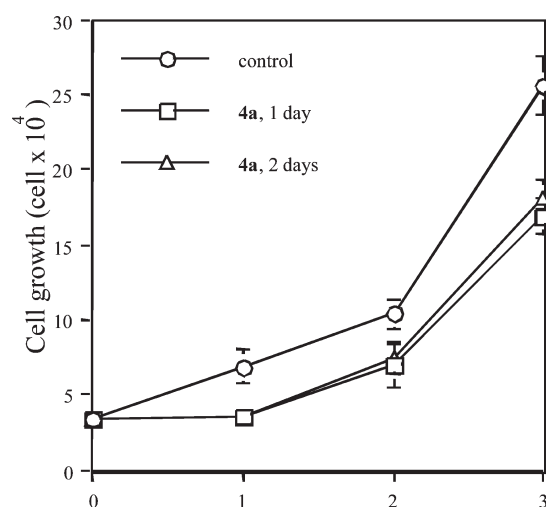


Figure 9. HeLaS-3 cell growth in the presence of 50 μM **4a**. For experimental details, see Experimental Section: (●) control, (□) 1 day, and (Δ) 2 days in the presence of **4a**.

entering the cell, **4a** is able to reduce the amount of phosphorylated Ado, although less efficiently than with the isolated cloned enzyme.

Effect of **4a on Cell Cultures.** To evaluate the effects of **4a** on cellular growth and viability, we exposed K562 (chronic myeloid leukemia cells) to various concentrations of the compound. Cell viability was measured by the dye exclusion assay described in the Experimental Section.

For comparison, we also determined the effect of 2',3'-dideoxycytidine (ddCyd), a compound known to affect cell growth and viability. As shown in Figure 8, **4a** inhibits cell growth and the drug concentration that inhibits the 50% of cell growth is 1 μM , a value comparable to that of ddCyd (0.8 μM). In both cases the compound blocks but does not kill the cells, since no blue stained cell was counted.

In order to study the effect of **4a** on cell growth, we incubated HeLaS-3 cells for 2 days in the presence of the compound (50 μM). We then washed the cells and left them to grow in fresh medium for an additional day. We found that once cells were washed and incubated in fresh medium, the inhibitory effect of **4a** on cells was maintained for the first 24 h while at later times cells rapidly recovered their normal growth rate (Figure 9).

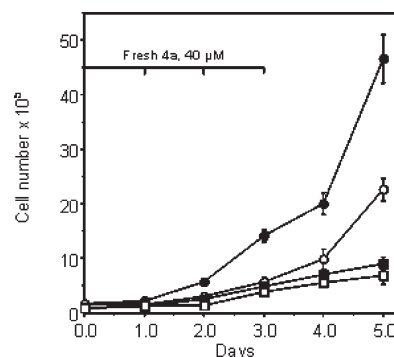


Figure 10. HeLaS-3 (●, ○) and Cen3tel (■, □) cell growth in the presence of 40 μM **4a**. For experimental details, see Experimental Section: (●, ■) control; (○, □) 3 days in the presence of **4a**.

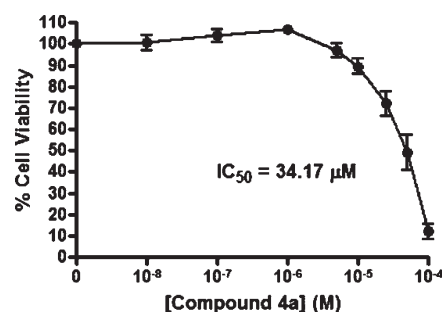


Figure 11. HL-60 cell viability in the presence of vehicle (0.1% (v/v) DMSO) or a range of concentrations of **4a** as described in the Experimental Section. Values represent the mean \pm SEM for three independent experiments.

Interestingly, we found that the cytostatic effect of the compound did not last more than 24–48 h even when HeLaS-3 cells and Cen3tel (fibroblast) cells³⁶ were incubated longer than 48 h, in presence of 40 μM **4a** freshly added every 24 h, as well (Figure 10).

This fact would suggest that cells, after a short period in which they are sensitive to the compound, are able to overcome the inhibitory effect by specific mechanisms that may involve induction of metabolic inactivation, increase of *hAK* activity, or other mechanisms of resistance. In order to evaluate these possibilities, we cultivated HeLaS-3 cells for 3 days in the presence of the drug (40 μM , added fresh every 24 h) and then we prepared cell crude extract as described in the Experimental Section. Extracts from treated and untreated cells were thus tested *in vitro* for both *hAK* and **4a** metabolizing activity. Our results demonstrated that **4a** is not degraded when incubated up to 20 h at 37 $^{\circ}\text{C}$ in the presence of crude extract, and no difference could be observed in *hAK* activity between **4a** treated and untreated cells (data not shown). This suggests that another mechanism is involved in the **4a** resistance in cells incubated 24–48 h in the presence of the compound.

We also performed cell viability assays in human promyelocytic leukemia HL-60 cells. The cells were treated with different concentrations of compound **4a** for 72 h. As highlighted in Figure 11, we determined that **4a** was effective in reducing cell viability with an IC_{50} of 34.17 μM .

We then explored if this reduction in HL60 cell viability occurred as a result of apoptosis. We analyzed the DNA content of the cells by flow cytometry. Cells found in the sub- G_0/G_1 peak

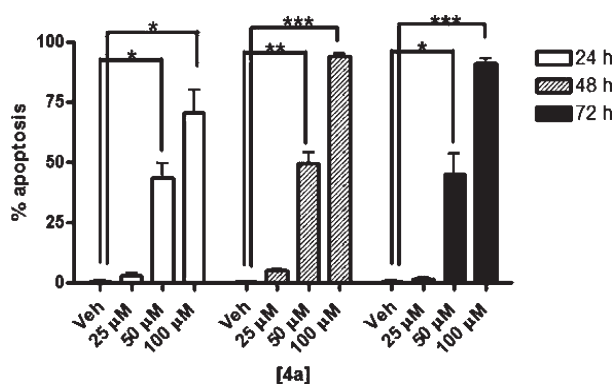


Figure 12. Effect of **4a** on apoptosis. Cells were treated with vehicle (0.1% DMSO) (Veh) or 25–100 μM **4a** for 24, 48, and 72 h. Their DNA content was then analyzed as described in the Experimental Section. Cells with less than 2N DNA content were deemed apoptotic. Values represent the mean \pm SEM for three independent experiments. (*) $P < 0.05$, (**) $P < 0.005$, and (***) $P < 0.0005$ were considered statistically significant using paired Student's t -tests.

Table 5. Percentage of Inhibition of ADA for Compounds **4a**, **4c**, **4g**, **4j**, and **4q**

compd	% inhibition (100 μM) ^a
4a	15 \pm 2
4c	6.5 \pm 0.7
4g	2.7 \pm 0.2
4j	13 \pm 1.9
4q	16 \pm 3

^a Percentage inhibition values of ADA activity at 100 μM . Values are the mean \pm SEM of two determinations carried out in triplicate.

Table 6. Cytotoxic Effect on 3T3 Cells Expressed as IC_{50} for Compounds **4a**, **4c**, **4g**, **4k**, and **4l**^a

compd	IC_{50} (μM)
4a	117.5
4c	97.8
4g	44.6
4k	47.6
4l	43.5

^a Each value is the mean of three determinations. SEM is $\leq 10\%$.

contained less than 2N DNA content and were considered apoptotic. After 24 h of treatment, 50 and 100 μM **4a** induced statistically significant increases in percent apoptosis, 44% and 70%, respectively, compared to 0.8% in vehicle-treated controls (Figure 12). After 48 h of treatment, the number of cells undergoing apoptosis further increased to over 90% following 100 μM **4a** compared to 0.7% in controls. Hence, we concluded that **4a** can function as a proapoptotic agent in HL-60 leukemia cells.

Effect of Pyrrolobenzoxa(thia)zepinones on Adenosine Deaminase (ADA) Activity. Besides AK, ADA is the other Ado metabolic enzyme present in cells. ADA catalyzes the irreversible Ado deamination to inosine. The role of AK is predominant in the physiological inactivation of Ado because of its higher affinity for the nucleoside (lower K_m).^{37,38} However, several studies have identified ADA inhibitors as potentiators of Ado induced cell

death or apoptosis.^{15,39} In order to assess the selectivity of our non-nucleoside *hAK* inhibitors, we also evaluated their ability to inhibit ADA. The enzymatic assay was performed on compounds **4a**, **4c**, **4g**, **4j**, and **4q** (for details see Experimental Section). Data reveal the almost complete lack of activity of these molecules (Table 5), confirming the selectivity of the compounds for *hAK*. These data allow us to exclude the inhibition of ADA by **4a** as the causative effect of apoptosis.

Cytotoxicity Studies. Cytotoxicity assays were performed to establish the effect of **4a**, **4c**, **4g**, **4k**, and **4l** on cell proliferation in vitro. IC_{50} values on 3T3 murine cell line are given in Table 6 (for details see the Experimental Section). The data confirm a low cytotoxic potential for the tested compounds.

CONCLUSIONS

By a screening approach, we identified a new class of non-nucleoside inhibitors of *hAK* with no affinity for ADA. The described compounds are characterized by structural features not reminiscent of the nucleoside structure. Through specific biological investigation we also demonstrated that the compounds were noncompetitive with both Ado and MgATP^{2-} . Thus, these benzoxa(thia)zepinones represent the first example of novel non-nucleoside noncompetitive inhibitors of *hAK* behaving as allosteric modulators of the human enzyme. This hypothesis was investigated by in silico studies that allowed us to propose a putative allosteric binding site for our molecules. The SAR trends experimentally determined for our compounds on the human enzyme could nicely be explained by the identified interaction in the postulated allosteric pocket. To explore the role of *hAK* in cell proliferation, we performed studies on living cells, highlighting that **4a** does not show significant adverse effect on short-term DNA synthesis. Furthermore, our lead compound **4a**, although it slightly inhibits short-term RNA synthesis, shows a cytostatic effect on different tumor cell lines, with almost no cytotoxic effect on normal cells.

In line with the described role played by Ado in the apoptotic pathway, suggesting a potential role for *hAK* inhibitors in cancer therapy, we also tested **4a** to evaluate its biological activity on leukemic (HL-60) cells. These studies demonstrated that **4a** potently reduced HL-60 cell viability ($\text{IC}_{50} = 34.17 \mu\text{M}$) by acting as a potent proapoptotic agent.

EXPERIMENTAL SECTION

Chemistry. Reagents were purchased from Aldrich and were used as received. Reaction progress was monitored by TLC using Merck silica gel 60 F₂₅₄ (0.040–0.063 mm) with detection by UV. Merck silica gel 60 (0.040–0.063 mm) was used for column chromatography.

Melting points were determined in Pyrex capillary tubes using an Electrothermal 8103 apparatus and are uncorrected. ¹H NMR and ¹³C NMR spectra were recorded on Bruker 200 MHz or Varian 300 MHz spectrometer with TMS as internal standard. Splitting patterns are described as singlet (s), doublet (d), triplet (t), quartet (q), and broad (br). The values of chemical shifts (δ) are given in ppm and coupling constants (J) in hertz (Hz).

ES-MS and APCI-MS spectra were obtained from an Agilent 1100 series LC/MSD spectrometer and from a LCQDeca-THERMOFINNIGAN spectrometer.

Elemental analyses were performed in a Perkin-Elmer 240C elemental analyzer, and the results were within $\pm 0.4\%$ of the theoretical values, unless otherwise noted.

Yields refer to purified products and are not optimized. All moisture-sensitive reactions were performed under argon atmosphere using oven-dried

glassware and anhydrous solvents. All the organic layers were dried using anhydrous sodium sulfate.

HPLC analytical chiral separation was performed by an AS Chiralpack analytical column (0.46 cm × 25 cm). The column used for the semipreparative separation was a Chiralpack AS (1 cm × 25 cm) containing as chiral stationary phase amylose tris[(*S*)- α -methylbenzylcarbamate] coated on 10 μ m silica gel. Before and after use, column functionality was tested with *trans*-stilbene oxide as standard compound. All runs were performed in isocratic mode at 25 °C with detection at 254 nm. Eluents were degassed by ultrasound treatment. Sample solutions for semipreparative separation (approximately 1 mg/mL) were prepared by dissolving the analytes in the eluent and filtering through 0.45 μ m Acrodisc filters. The injection volume was 100 μ L.

Optical rotation values were measured at room temperature operating at λ = 589 nm, corresponding to the sodium D line, and were determined in a Perkin-Elmer polarimeter using a microcell (1 mg sensitivity) containing the compound dissolved in 1 mL of chloroform.

For biological tests analytical grade reagents were exclusively used. Bacterial media components were from Difco. Ni-NTA Superflow resin was from Qiagen. Restriction and modification enzymes were from Promega, Sigma, or Roche Molecular Biochemicals. Isopropylthio- β -D-galactoside (IPTG) was from Sigma. [³H]Ado, 22 Ci/mmol, was from Amersham.

(\pm)-6-Ethyl-6-[4-[(phenylthio)methyl]phenyl]-6,7-dihydrobenzo[b]pyrrolo[1,2-d][1,4]oxazepin-7-one (**4a**). Sodium hydride (60% suspension in mineral oil, 22 mg, 0.550 mmol) was added to a solution of thiophenol (50 mg, 0.530 mmol) in 3.0 mL of dry THF. After being stirred for 2 h at room temperature under argon atmosphere, a solution of the bromide **5** (200 mg, 0.500 mmol) in dry THF (4.0 mL) was added. The mixture was stirred at room temperature for 12 h. After the reaction was quenched with a saturated aqueous solution of ammonium chloride, THF was removed under reduced pressure. DCM was added, and the solution was washed with brine. The combined organic layers were dried over sodium sulfate, filtered, and concentrated. The crude product was purified by means of flash chromatography (EtOAc/*n*-hexane 1:10), affording **4a** as an amorphous white solid (72% yield): ¹H NMR (200 MHz, CDCl₃) δ 1.03 (t, 3H, *J* = 7.5 Hz), 2.38 (m, 2H), 3.99 (s, 2H), 6.45 (m, 1H), 6.91–7.28 (m, 15H); ¹³C NMR (75 MHz, CDCl₃) δ 9.1, 33.0, 37.0, 95.4, 112.5, 121.2, 122.7, 126.2, 126.4, 126.5, 126.7, 126.8, 127.8, 127.9, 128.1, 128.2, 129.3, 129.4, 129.5, 129.6, 133.6, 134.0, 136.5, 137.1, 138.4, 146.4, 191.8. Anal. (C₂₇H₂₃NO₂S) C, H, N.

(\pm)-6-Ethyl-6-[4-[(2-fluorophenylthio)methyl]phenyl]-6,7-dihydrobenzo[b]pyrrolo[1,2-d][1,4]oxazepin-7-one (**4b**). Compound **4b** was obtained following the same procedure described for compound **4a**. Purification was performed by means of flash chromatography (EtOAc/*n*-hexane 1:9). Title compound was obtained as a pale yellow oil (61% yield): ¹H NMR (200 MHz, CDCl₃) δ 1.02 (t, 3H, *J* = 7.2 Hz) 2.37 (m, 2H), 3.98 (s, 2H), 6.45 (m, 1H), 6.92–7.28 (m, 14H). Anal. (C₂₇H₂₂FNO₂S) C, H, N.

(\pm)-6-Ethyl-6-[4-[(2-chlorophenylthio)methyl]phenyl]-6,7-dihydrobenzo[b]pyrrolo[1,2-d][1,4]oxazepin-7-one (**4c**). Compound **4c** was obtained following the same procedure described for compound **4a**. Purification was performed by means of flash chromatography (EtOAc/*n*-hexane 1:9). Title compound was obtained as a pale yellow oil (57% yield): ¹H NMR (300 MHz, CDCl₃) δ 1.02 (t, 3H, *J* = 7.3 Hz), 2.38 (m, 2H), 4.04 (s, 2H), 6.45 (m, 1H), 6.92–7.37 (m, 14H); ¹³C NMR (75 MHz, CDCl₃) δ 8.6, 32.5, 37.3, 96.0, 112.0, 120.8, 121.9, 125.5, 125.8, 126.2, 127.2, 127.3, 128.0, 128.8 (2C), 129.8, 129.9, 134.0, 134.1, 134.2, 135.6, 136.6, 137.7, 146.8, 192.8. Anal. (C₂₇H₂₂ClNO₂S) C, H, N.

(\pm)-6-Ethyl-6-[4-[(3-methylphenylthio)methyl]phenyl]-6,7-dihydrobenzo[b]pyrrolo[1,2-d][1,4]oxazepin-7-one (**4d**). Compound **4d** was obtained following the same procedure described for compound **4a**. Purification was performed by means of flash chromatography (diethyl ether/*n*-hexane 1:4). Title compound was obtained as a pale yellow

oil (71% yield): ¹H NMR (200 MHz, CDCl₃) δ 1.03 (t, 3H, *J* = 7.5 Hz), 2.38 (m, 2H), 3.35 (s, 3H), 4.20 (s, 2H), 6.44 (m, 1H), 6.91–7.36 (m, 14H). Anal. (C₂₈H₂₅NO₂S) C, H, N.

(\pm)-6-Ethyl-6-[4-[(3-fluorophenylthio)methyl]phenyl]-6,7-dihydrobenzo[b]pyrrolo[1,2-d][1,4]oxazepin-7-one (**4e**). Compound **4e** was obtained following the same procedure described for compound **4a**. Purification was performed by means of flash chromatography (EtOAc/*n*-hexane 1:9). Title compound was obtained as a pale yellow oil (66% yield): ¹H NMR (200 MHz, CDCl₃) δ 1.03 (t, 3H, *J* = 7.5 Hz), 2.38 (m, 2H), 4.00 (s, 2H), 6.43 (m, 1H), 6.91–7.35 (m, 14H). Anal. (C₂₇H₂₂FNO₂S) C, H, N.

(\pm)-6-Ethyl-6-[4-[(3-chlorophenylthio)methyl]phenyl]-6,7-dihydrobenzo[b]pyrrolo[1,2-d][1,4]oxazepin-7-one (**4f**). Compound **4f** was obtained following the same procedure described for compound **4a**. Purification was performed by means of flash chromatography (EtOAc/*n*-hexane 1:9). Title compound was obtained as a pale yellow oil (71% yield): ¹H NMR (200 MHz, CDCl₃) δ 1.03 (t, 3H, *J* = 7.5 Hz), 2.38 (m, 2H), 4.00 (s, 2H), 6.40 (m, 1H), 6.90–7.31 (m, 14H). Anal. (C₂₇H₂₂ClNO₂S) C, H, N.

(\pm)-6-Ethyl-6-[4-[(3-trifluoromethylphenylthio)methyl]phenyl]-6,7-dihydrobenzo[b]pyrrolo[1,2-d][1,4]oxazepin-7-one (**4g**). Compound **4g** was obtained following the same procedure described for compound **4a**. Purification was performed by means of flash chromatography (EtOAc/*n*-hexane 1:9). Title compound was obtained as a pale yellow oil (65% yield): ¹H NMR (200 MHz, CDCl₃) δ 1.02 (t, 3H, *J* = 7.5 Hz), 2.38 (m, 2H), 4.03 (s, 2H), 6.45 (m, 1H), 6.91–7.47 (m, 14H). Anal. (C₂₈H₂₂F₃NO₂S) C, H, N.

(\pm)-6-Ethyl-6-[4-[(3-methoxyphenylthio)methyl]phenyl]-6,7-dihydrobenzo[b]pyrrolo[1,2-d][1,4]oxazepin-7-one (**4h**). Compound **4h** was obtained following the same procedure described for compound **4a**. Purification was performed by means of flash chromatography (EtOAc/*n*-hexane 1:9). Title compound was obtained as a pale yellow oil (73% yield): ¹H NMR (300 MHz, CDCl₃) δ 1.03 (t, 3H, *J* = 7.2 Hz), 2.40 (m, 2H), 3.71 (s, 3H), 3.86 (s, 2H), 6.46 (m, 1H), 6.75 (m, 2H), 6.94–7.23 (m, 7H), 7.25–7.33 (m, 5H). Anal. (C₂₈H₂₅NO₃S) C, H, N.

(\pm)-6-Ethyl-6-[4-[(3-trifluoromethoxyphenylthio)methyl]phenyl]-6,7-dihydrobenzo[b]pyrrolo[1,2-d][1,4]oxazepin-7-one (**4i**). Compound **4i** was obtained following the same procedure described for compound **4a**. Purification was performed by means of flash chromatography (EtOAc/*n*-hexane 1:9). Title compound was obtained as a pale yellow oil (77% yield): ¹H NMR (300 MHz, CDCl₃) δ 1.01 (t, 3H, *J* = 7.3 Hz), 2.36 (m, 2H), 4.01 (s, 2H), 6.42 (m, 1H), 6.87–7.33 (m, 14H). Anal. (C₂₈H₂₂F₃NO₃S) C, H, N.

(\pm)-6-Ethyl-6-[4-[(4-fluorophenylthio)methyl]phenyl]-6,7-dihydrobenzo[b]pyrrolo[1,2-d][1,4]oxazepin-7-one (**4j**). Compound **4j** was obtained following the same procedure described for compound **4a**. Purification was performed by means of flash chromatography (petroleum ether 40–60 °C/DCM 2:1). Title compound was obtained as a pale yellow oil (71% yield): ¹H NMR (300 MHz, CDCl₃) δ 1.04 (t, 3H, *J* = 7.3 Hz), 2.40 (m, 2H), 3.91 (s, 2H), 6.46 (m, 1H), 6.84–7.29 (m, 14H). Anal. (C₂₇H₂₂FNO₂S) C, H, N.

(\pm)-6-Ethyl-6-[4-[(4-bromophenylthio)methyl]phenyl]-6,7-dihydrobenzo[b]pyrrolo[1,2-d][1,4]oxazepin-7-one (**4k**). Compound **4k** was obtained following the same procedure described for compound **4a**. Purification was performed by means of flash chromatography (EtOAc/*n*-hexane 1:9). Title compound was obtained as a pale yellow oil (70% yield): ¹H NMR (300 MHz, CDCl₃) δ 1.03 (t, 3H, *J* = 7.3 Hz), 2.39 (m, 2H), 4.00 (s, 2H), 6.43 (m, 1H), 6.88–7.30 (m, 14H). Anal. (C₂₇H₂₂BrNO₂S) C, H, N.

1,2-bis-(4-iodophenyl)disulfane (**7**). To a solution of 4-amino-benzenethiol (**6a**) (192 mg, 1.53 mmol) in 1.4 mL of water, cooled to 0 °C, concentrated HCl (1.5 mL), concentrated H₂SO₄ (600 μ L), and sodium nitrite (126 mg, 1.840 mmol) were added. After the mixture was

stirred at 0 °C for 30 min urea (9 mg, 0.150 mmol) was added. The mixture was stirred for another 15 min. A solution of potassium iodide (508 mg, 3.060 mmol) in 30 mL of water was added, and the resulting mixture was stirred for 5 h at 0 °C. The disappearance of the starting material was checked by thin layer chromatography (petroleum ether 40–60 °C). The mixture was then taken up with EtOAc. The aqueous phase was separated and extracted with EtOAc (3 × 80 mL). The combined organic layers were washed with water, dried over sodium sulfate, filtered, and evaporated. The residue was purified by means of flash column chromatography (petroleum ether 40–60 °C). Title compound was obtained with a 62% yield. Spectroscopic data of title compound are consistent with those reported in the literature.⁴⁰

4-Iodobenzenethiol (9a). To an ice-cooled solution of compound 7 in 2 mL of MeOH, sodium borohydride (18 mg, 0.480 mmol) was added. After the mixture was stirred at 0 °C for 3 h water was added and MeOH was removed under reduced pressure. HCl (12 N) was added to the mixture until a white precipitate formed, then EtOAc was added. The aqueous phase was separated and extracted with EtOAc (3 × 20 mL). The combined organic phases were dried over sodium sulfate, filtered, and concentrated. The compound was carried on without further purification (84% yield). Spectroscopic data of the title compound are consistent with those reported in the literature.⁴¹

(±)-6-Ethyl-6-[4-[(4-iodophenylthio)methyl]phenyl]-6,7-dihydrobenzo[b]pyrrolo[1,2-d][1,4]oxazepin-7-one (4l). Compound 4l was obtained following the same procedure described for compound 4a. Purification was performed by means of flash chromatography (EtOAc/*n*-hexane 1:1). Title compound was obtained as a pale yellow oil (47% yield): ¹H NMR (300 MHz, CDCl₃) δ 1.05 (t, 3H, *J* = 7.3 Hz), 2.26–2.51 (m, 2H), 3.98 (s, 2H), 6.47 (m, 1H), 6.89–7.51 (m, 14H); ¹³C NMR (75 MHz, CDCl₃) δ 8.6, 32.7, 38.6, 91.7, 95.9, 112.1, 120.9, 121.9, 125.5, 125.9, 126.2, 127.1, 128.0, 128.8, 131.9, 134.0, 134.3, 136.2, 137.3, 137.6, 137.9, 146.8, 192.8. Anal. (C₂₇H₂₂INO₂S) C, H, N.

(±)-6-Ethyl-6-[4-[(4-nitrophenylthio)methyl]phenyl]-6,7-dihydrobenzo[b]pyrrolo[1,2-d][1,4]oxazepin-7-one (4m). Compound 4m was obtained following the same procedure described for compound 4a. Purification was performed by means of flash chromatography (EtOAc/*n*-hexane 1:4). Title compound was obtained as a pale yellow oil (44% yield): ¹H NMR (300 MHz, CDCl₃) δ 1.01 (t, 3H, *J* = 7.4 Hz), 2.35 (m, 2H), 4.03 (s, 2H), 6.44 (m, 1H), 6.88–7.32 (m, 14H). Anal. (C₂₇H₂₂N₂O₄S) C, H, N.

(±)-6-Ethyl-6-[4-[(4-trifluoromethoxyphenylthio)methyl]phenyl]-6,7-dihydrobenzo[b]pyrrolo[1,2-d][1,4]oxazepin-7-one (4n). Compound 4n was obtained following the same procedure described for compound 4a. Purification was performed by means of flash chromatography (EtOAc/*n*-hexane 1:9). Title compound was obtained as a pale yellow oil (85% yield): ¹H NMR (300 MHz, CDCl₃) δ 1.03 (t, 3H, *J* = 7.3 Hz), 2.40 (m, 2H), 3.98 (s, 2H), 6.44 (m, 1H), 6.90–7.35 (m, 14H). Anal. (C₂₈H₂₂F₃NO₃S) C, H, N.

(±)-6-Ethyl-6-[4-[(4-methoxyphenylthio)methyl]phenyl]-6,7-dihydrobenzo[b]pyrrolo[1,2-d][1,4]oxazepin-7-one (4o). Compound 4o was obtained following the same procedure described for compound 4a. Purification was performed by means of flash chromatography (EtOAc/*n*-hexane 1:7). Title compound was obtained as a pale yellow oil (55% yield): ¹H NMR (300 MHz, CDCl₃) δ 1.05 (t, 3H, *J* = 7.3 Hz), 2.40 (m, 2H), 3.78 (s, 3H), 3.86 (s, 2H), 6.46 (m, 1H), 6.72 (m, 2H), 6.94–7.12 (m, 7H), 7.22–7.29 (m, 5H). Anal. (C₂₈H₂₅NO₃S) C, H, N.

(±)-6-Ethyl-6-[4-[(2-trimethylsilyl)ethynyl]phenylthio]methyl]phenyl]-6,7-dihydrobenzo[b]pyrrolo[1,2-d][1,4]oxazepin-7-one (4p). In a sealed tube containing a suspension of compound 4l (54 mg, 0.098 mmol) in TEA (1 mL) with dichlorobis-(triphenylphosphine)palladium(II) (3 mg, 0.005 mmol) and copper iodide (1 mg, 0.005 mmol), trimethylsilylacetylene (17 μL, 0.12 mmol) was added dropwise. The resulting mixture was stirred for 12 h at room temperature. After that time the solution was diluted with water and

extracted with diethyl ether (3 × 10 mL). The combined organic layers were dried over sodium sulfate, filtered, and concentrated. Purification was performed by means of flash chromatography (*n*-hexane/DCM 1:1). Title compound was obtained as a pale yellow oil (85% yield): ¹H NMR (300 MHz, CDCl₃) δ 0.26 (s, 9H), 1.05 (t, 3H, *J* = 7.0 Hz), 2.29–2.51 (m, 2H), 4.01 (s, 2H), 6.47 (s, 1H), 6.93–7.30 (m, 14H); ¹³C NMR (75 MHz, CDCl₃) δ 0.2, 8.6, 32.7, 38.3, 95.0, 95.9, 104.9, 112.0, 120.8, 121.2, 121.8, 125.5, 125.8, 126.2, 127.1, 128.0, 128.7, 129.3, 132.4, 133.9, 134.3, 137.2 (2C), 137.6, 146.8, 192.7. Anal. (C₃₂H₃₁NO₂SSi) C, H, N.

(±)-6-Ethyl-6-[4-[(4-ethynylphenylthio)methyl]phenyl]-6,7-dihydrobenzo[b]pyrrolo[1,2-d][1,4]oxazepin-7-one (4q). To a solution of 4p (37 mg, 0.07 mmol) in 2 mL of MeOH and 360 μL of THF, potassium carbonate (10 mg 0.08 mmol) was added. The resultant suspension was stirred for 45 min. Then the solution was diluted with water and extracted with diethyl ether (3 × 10 mL). The combined organic layers were dried over sodium sulfate, filtered, and concentrated. Purification was performed by means of flash chromatography (EtOAc/*n*-hexane 1:8). Title compound was obtained as a pale yellow oil (75% yield): ¹H NMR (300 MHz, CDCl₃) δ 1.04 (t, 3H, *J* = 7.3 Hz), 2.29–2.51 (m, 2H), 3.09 (s, 1H), 4.03 (s, 2H), 6.46 (s, 1H), 6.92–7.33 (m, 14H); ¹³C NMR (75 MHz, CDCl₃) δ 8.6, 14.4, 32.6, 38.1, 77.9, 83.5, 95.9, 112.0, 120.8, 121.6, 125.5, 125.8, 126.2, 127.1, 128.0 (2C), 128.7 (2C), 129.2 (2C), 132.6, 134.0, 134.3, 137.1, 137.6, 137.8, 146.8, 192.7. Anal. (C₂₉H₂₃NO₂S) C, H, N.

(±)-6-Ethyl-6-[4-[(2-methyl-6-chlorophenylthio)methyl]phenyl]-6,7-dihydrobenzo[b]pyrrolo[1,2-d][1,4]oxazepin-7-one (4r). Compound 4r was obtained following the same procedure described for compound 4a. Purification was performed by means of flash chromatography (EtOAc/*n*-hexane 1:9). Title compound was obtained as a pale yellow oil (64% yield): ¹H NMR (300 MHz, CDCl₃) δ 1.00 (t, 3H, *J* = 7.3 Hz), 2.11 (s, 3H), 2.34 (m, 2H), 3.88 (s, 2H), 6.45 (m, 1H), 6.91–7.36 (m, 13H). Anal. (C₂₈H₂₄ClNO₂S) C, H, N.

(±)-6-Ethyl-6-[4-[(2,6-dichlorophenylthio)methyl]phenyl]-6,7-dihydrobenzo[b]pyrrolo[1,2-d][1,4]oxazepin-7-one (4s). Compound 4s was obtained following the same procedure described for compound 4a. Purification was performed by means of flash chromatography (diethyl ether/petroleum ether 40–60 °C 1:8). Title compound was obtained as an amorphous white solid (77% yield): ¹H NMR (300 MHz, CDCl₃) δ 1.00 (t, 3H, *J* = 7.3 Hz), 2.34 (m, 2H), 4.00 (s, 2H), 6.45 (m, 1H), 6.96–7.14 (m, 6H), 7.21–7.47 (m, 7H). Anal. (C₂₇H₂₁Cl₂NO₂S) C, H, N.

Resolution of (±)-6-Ethyl-6-[4-[(2,6-dichlorophenylthio)methyl]phenyl]-6,7-dihydrobenzo[b]pyrrolo[1,2-d][1,4]oxazepin-7-one (4s). A sample solution of (±)-4s (1 mg/mL) was prepared by dissolving the compound in the eluent (*n*-hexane 98%, EtOH 2%, TEA 0.2%) and filtering through 0.45 μm Acrodisc filters. The injection volume was 100 μL. The racemic mixture was resolved at room temperature using *n*-hexane 98%, EtOH 2%, and TEA 0.2% as eluent (flow rate of the mobile phase 3.8 mL/min). The effluent was monitored at (λ) 589 nm, and the enantiomers (–)-4s and (+)-4s were eluted with retention times of 13.5 and 15.08 min, respectively. Fractions were collected by using a Vario2000 fraction collector, and solutions were dried with a vacuum pump. Purity of the enantiomers was evaluated by analytical HPLC using the same mobile phase (flow rate of 0.8 mL/min), and the enantiomers (–)-4s and (+)-4s were eluted with retention times of 13.8 and 15.30 min, respectively. (–)-4s and (+)-4s ¹H NMR data are identical to those of (±)-4s. (–)-4s [α]_D²⁰ –18.7° (c 0.4, chloroform). Anal. (C₂₇H₂₁Cl₂NO₂S) C, H, N. (+)-4s [α]_D²⁰ +18.5° (c 0.4, chloroform). Anal. (C₂₇H₂₁Cl₂NO₂S) C, H, N.

(±)-6-Ethyl-6-[4-[(2,3-dichlorophenylthio)methyl]phenyl]-6,7-dihydrobenzo[b]pyrrolo[1,2-d][1,4]oxazepin-7-one (4t). Compound 4t was obtained following the same procedure described for compound 4a. Purification was performed by means of flash chromatography (EtOAc/*n*-hexane 1:5). Title compound was obtained as an

amorphous white solid (54% yield): ^1H NMR (300 MHz, CDCl_3) δ 1.02 (t, 3H, $J = 7.3$ Hz), 2.38 (m, 2H), 4.06 (s, 2H), 6.45 (m, 1H), 6.97–7.14 (m, 5H), 7.21–7.38 (m, 8H). Anal. ($\text{C}_{27}\text{H}_{21}\text{Cl}_2\text{NO}_2\text{S}$) C, H, N.

(\pm)-6-Ethyl-6-[4-[(2,5-dichlorophenylthio)methyl]phenyl]-6,7-dihydrobenzo[b]pyrrolo[1,2-d][1,4]oxazepin-7-one (4u). Compound 4u was obtained following the same procedure described for compound 4a. Purification was performed by means of flash chromatography (DCM/petroleum ether 40–60 °C 1:2). Title compound was obtained as an amorphous white solid (66% yield): ^1H NMR (300 MHz, CDCl_3) δ 1.02 (t, 3H, $J = 7.2$ Hz), 2.38 (m, 2H), 4.05 (s, 2H), 6.45 (m, 1H), 6.94–7.13 (m, 5H), 7.21–7.35 (m, 8H). Anal. ($\text{C}_{27}\text{H}_{21}\text{Cl}_2\text{NO}_2\text{S}$) C, H, N.

(\pm)-6-Ethyl-6-[4-[(2,4-dichlorophenylthio)methyl]phenyl]-6,7-dihydrobenzo[b]pyrrolo[1,2-d][1,4]oxazepin-7-one (4v). Compound 4v was obtained following the same procedure described for compound 4a. Purification was performed by means of flash chromatography (diethyl ether/petroleum ether 40–60 °C 1:8). Title compound was obtained as an amorphous white solid (74% yield): ^1H NMR (300 MHz, CDCl_3) δ 1.03 (t, 3H, $J = 7.3$ Hz), 2.38 (m, 2H), 4.03 (s, 2H), 6.46 (m, 1H), 6.94–7.37 (m, 13H). Anal. ($\text{C}_{27}\text{H}_{21}\text{Cl}_2\text{NO}_2\text{S}$) C, H, N.

(\pm)-6-Ethyl-6-[4-[(3,4-dichlorophenylthio)methyl]phenyl]-6,7-dihydrobenzo[b]pyrrolo[1,2-d][1,4]oxazepin-7-one (4w). Compound 4w was obtained following the same procedure described for compound 4a. Purification was performed by means of flash chromatography (diethyl ether/petroleum ether 40–60 °C 1:8). Title compound was obtained as an amorphous white solid (72% yield): ^1H NMR (300 MHz, CDCl_3) δ 1.01 (t, 3H, $J = 7.3$ Hz), 2.37 (m, 2H), 4.01 (s, 2H), 6.45 (m, 1H), 6.93–7.13 (m, 6H), 7.21–7.46 (m, 7H). Anal. ($\text{C}_{27}\text{H}_{21}\text{Cl}_2\text{NO}_2\text{S}$) C, H, N.

(\pm)-6-Ethyl-6-[4-[(2,4-difluorophenylthio)methyl]phenyl]-6,7-dihydrobenzo[b]pyrrolo[1,2-d][1,4]oxazepin-7-one (4x). Compound 4x was obtained following the same procedure described for compound 4a. Purification was performed by means of flash chromatography (diethyl ether/*n*-hexane 1:9). Title compound was obtained as a pale yellow oil (53% yield): ^1H NMR (300 MHz, CDCl_3) δ 1.00 (t, 3H, $J = 7.3$ Hz), 2.36 (m, 2H), 3.90 (s, 2H), 6.44 (m, 1H), 6.66 (m, 1H), 6.80 (m, 1H), 6.92–7.32 (m, 11H). Anal. ($\text{C}_{27}\text{H}_{21}\text{F}_2\text{NO}_2\text{S}$) C, H, N.

(\pm)-6-Ethyl-6-[4-[(2-chloro-4-fluorophenylthio)methyl]phenyl]-6,7-dihydrobenzo[b]pyrrolo[1,2-d][1,4]oxazepin-7-one (4y). Compound 4y was obtained following the same procedure described for compound 4a. Purification was performed by means of flash chromatography (diethyl ether/petroleum ether 40–60 °C 1:9). Title compound was obtained as an amorphous white solid (67% yield): ^1H NMR (300 MHz, CDCl_3) δ 1.02 (t, 3H, $J = 7.3$ Hz), 2.37 (m, 2H), 4.02 (s, 2H), 6.41 (m, 1H), 6.91–7.36 (m, 13H). Anal. ($\text{C}_{27}\text{H}_{21}\text{ClFNO}_2\text{S}$) C, H, N.

(\pm)-6-Ethyl-6-[4-[(3-chloro-4-fluorophenylthio)methyl]phenyl]-6,7-dihydrobenzo[b]pyrrolo[1,2-d][1,4]oxazepin-7-one (4z). Compound 4z was obtained following the same procedure described for compound 4a. Purification was performed by means of flash chromatography (EtOAc/petroleum ether 40–60 °C 1:9). Title compound was obtained as an amorphous white solid (65% yield): ^1H NMR (300 MHz, CDCl_3) δ 1.03 (t, 3H, $J = 7.3$ Hz), 2.34 (m, 2H), 4.00 (s, 2H), 6.38 (m, 1H), 6.88–7.32 (m, 13H). Anal. ($\text{C}_{27}\text{H}_{21}\text{ClFNO}_2\text{S}$) C, H, N.

(\pm)-6-Ethyl-6-[4-[(2,5-dimethoxyphenylthio)methyl]phenyl]-6,7-dihydrobenzo[b]pyrrolo[1,2-d][1,4]oxazepin-7-one (4aa). Compound 4aa was obtained following the same procedure described for compound 4a. Purification was performed by means of flash chromatography (EtOAc/*n*-hexane 1:9). Title compound was obtained as a pale yellow oil (70% yield): ^1H NMR (300 MHz, CDCl_3) δ 1.01 (t, 3H, $J = 7.2$ Hz), 2.33 (m, 2H), 3.81 (s, 3H), 3.83 (s, 3H), 4.20 (s, 2H), 6.64 (m, 2H), 6.78 (m, 1H), 6.91 (m, 1H), 7.15–7.20 (m, 4H), 7.25–7.30 (m, 3H), 7.37 (m, 1H), 7.46 (m, 1H), 7.55 (m, 1H). Anal. ($\text{C}_{29}\text{H}_{27}\text{NO}_4\text{S}$) C, H, N.

2-Chloro-4-iodophenol (8). Starting from 4-amino-2-chlorophenol 6b the title compound was prepared according to the procedure described for 7. The crude was purified by means of flash chromatography (EtOAc/*n*-hexane 1:5) (55% yield). Spectroscopic data of the title compound are consistent with those reported in the literature.⁴²

O-2-Chloro-4-iodophenyl-*N,N*-dimethylcarbamothioate (10). A solution of compound 8 (124 mg, 0.490 mmol) in DMF (600 μL) was treated with DABCO (110 mg, 0.980 mmol) and dimethylthiocarbamyl chloride (96 mg, 0.780 mmol). The mixture was stirred at room temperature for 1 h. Then it was diluted with EtOAc and poured into ice-water. The layers were separated, and the aqueous phase was extracted with EtOAc (3 \times 50 mL). The combined organic extracts were washed with water and with brine. The combined organic layers were dried over sodium sulfate, filtered, and concentrated. The crude was purified by means of flash chromatography (EtOAc/*n*-hexane 1:5). Title compound was obtained with a 63% yield: ^1H NMR (300 MHz, CDCl_3) δ 3.37 (s, 3H), 3.45 (s, 3H), 6.89 (d, 1H, $J = 8.5$ Hz), 7.63 (d, 1H, $J = 8.5$ Hz), 7.76 (s, 1H); ^{13}C NMR (75 MHz, CDCl_3) δ 39.2, 43.8, 90.2, 127.1, 129.1, 136.8, 138.7, 150.2, 186.1.

S-2-Chloro-4-iodophenyl-*N,N*-dimethylcarbamothioate (11). A sealed tube containing compound 10 (105 mg, 0.31 mmol) was inserted into the cavity of the microwave apparatus and heated neat at 220 °C, employing a microwave power of 150 W for 10 min. After the mixture was cooled, the crude was taken up with DCM and purified by means of flash chromatography (DCM). Title compound was obtained with a 82% yield: ^1H NMR (300 MHz, CDCl_3) δ 3.03 (s, 3H), 3.10 (s, 3H), 7.28 (d, 1H, $J = 8.2$ Hz), 7.60 (d, 1H, $J = 8.2$ Hz), 7.84 (s, 1H); ^{13}C NMR (75 MHz, CDCl_3) δ 37.3, 96.1, 128.7, 136.6, 138.6, 139.3, 140.5, 164.7.

2-Chloro-4-iodobenzenethiol (9b). Compound 11 (87 mg, 0.250 mmol) was dissolved in EtOH (400 μL) and treated with 3 N aqueous KOH (292 μL). The mixture was heated at reflux for 3 h, and then it was allowed to cool to room temperature. After removal of EtOH under reduced pressure, the aqueous solution was acidified with 3 N HCl until pH \sim 3 and extracted with EtOAc (3 \times 100 mL). The combined organic layers were dried over sodium sulfate, filtered, and concentrated. The compound was used in the following step without further purification (80% yield): ^1H NMR (300 MHz, CDCl_3) δ 3.89 (s, 1H), 7.05 (d, 1H, $J = 8.2$ Hz), 7.43 (d, 1H, $J = 8.2$ Hz), 7.69 (s, 1H).

(\pm)-6-Ethyl-6-[4-[(2-chloro-4-iodophenylthio)methyl]phenyl]-6,7-dihydrobenzo[b]pyrrolo[1,2-d][1,4]oxazepin-7-one (4bb). Compound 4bb was obtained following the same procedure described for compound 4a. Purification was performed by means of flash chromatography (chloroform/*n*-hexane 1:1). Title compound was obtained as an amorphous white solid (55% yield): ^1H NMR (300 MHz, CDCl_3) δ 1.03 (t, 3H, $J = 7.3$ Hz), 2.27–2.50 (m, 2H), 4.03 (s, 2H), 6.45 (m, 1H), 6.77–7.40 (m, 12H), 7.67 (s, 1H); ^{13}C NMR (75 MHz, CDCl_3) δ 8.6, 29.9, 32.5, 37.1, 77.5, 90.2, 95.9, 112.0, 120.9, 121.9, 125.5, 125.9, 126.2, 127.1, 128.1, 128.8, 130.8, 133.9, 134.2, 134.8, 135.8, 136.2, 137.9, 146.8, 192.7. Anal. ($\text{C}_{27}\text{H}_{21}\text{ClINO}_2\text{S}$) C, H, N.

(\pm)-6-Ethyl-6-[4-[(2,3,5,6-tetrafluorophenylthio)methyl]phenyl]-6,7-dihydrobenzo[b]pyrrolo[1,2-d][1,4]oxazepin-7-one (4cc). Compound 4cc was obtained following the same procedure described for compound 4a. Purification was performed by means of flash chromatography (diethyl ether/*n*-hexane 1:9). Title compound was obtained as an amorphous white solid (45% yield): ^1H NMR (300 MHz, CDCl_3) δ 1.02 (t, 3H, $J = 7.3$ Hz), 2.36 (m, 2H), 4.02 (s, 2H), 6.42 (m, 1H), 6.86–7.35 (m, 11H). Anal. ($\text{C}_{27}\text{H}_{19}\text{F}_4\text{NO}_2\text{S}$) C, H, N.

(\pm)-6-Ethyl-6-[4-[(2-pyridylthio)methyl]phenyl]-6,7-dihydrobenzo[b]pyrrolo[1,2-d][1,4]oxazepin-7-one (4dd). Compound 4dd was obtained following the same procedure described for compound 4a. Purification was performed by means of flash chromatography (EtOAc/*n*-hexane 1:9). Title compound was obtained as a pale yellow oil (75% yield): ^1H NMR (200 MHz, CDCl_3) δ 1.03

(t, 3H, $J = 7.5$ Hz), 2.38 (m, 2H), 4.35 (s, 2H), 6.43 (m, 1H), 6.93–7.48 (m, 13H), 8.39 (m, 1H). Anal. ($C_{26}H_{22}N_2O_2S$) C, H, N.

(±)-6-Ethyl-6-[4-[(2-imidazolylthio)methyl]phenyl]-6,7-dihydrobenzo[*b*]pyrrolo[1,2-*d*][1,4]oxazepin-7-one (**4ee**). Compound **4ee** was obtained following the same procedure described for compound **4a**. Purification was performed by means of flash chromatography (EtOAc/*n*-hexane 4:6). Title compound was obtained as a pale yellow oil (78% yield): 1H NMR (200 MHz, $CDCl_3$) δ 1.02 (t, 3H, $J = 7.5$ Hz), 2.36 (m, 2H), 4.12 (s, 2H), 6.43 (t, 1H), 6.97–7.39 (m, 12H), 12.9 (br s, 1H). Anal. ($C_{24}H_{21}N_3O_2S$) C, H, N.

(±)-6-Ethyl-6-[4-[(2-pyrazylthio)methyl]phenyl]-6,7-dihydrobenzo[*b*]pyrrolo[1,2-*d*][1,4]oxazepin-7-one (**4ff**). Compound **4ff** was obtained following the same procedure described for compound **4a**. Purification was performed by means of flash chromatography (EtOAc/*n*-hexane 1:9). Title compound was obtained as a yellow oil (64% yield): 1H NMR (200 MHz, $CDCl_3$) δ 1.03 (t, 3H, $J = 7.5$ Hz), 2.39 (m, 2H), 4.08 (s, 2H), 6.44 (m, 1H), 6.91–7.36 (m, 10H), 8.59–8.63 (m, 3H). Anal. ($C_{25}H_{21}N_3O_2S$) C, H, N.

(±)-6-Ethyl-6-[4-[(2-pyrimidylthio)methyl]phenyl]-6,7-dihydrobenzo[*b*]pyrrolo[1,2-*d*][1,4]oxazepin-7-one (**4gg**). Compound **4gg** was obtained following the same procedure described for compound **4a**. Purification was performed by means of flash chromatography (EtOAc/*n*-hexane 1:9). Title compound was obtained as a yellow oil (69% yield): 1H NMR (200 MHz, $CDCl_3$) δ 1.01 (t, 3H, $J = 7.5$ Hz), 2.38 (m, 2H), 4.06 (s, 2H), 6.45 (m, 1H), 6.91–7.39 (m, 11H), 8.61–8.65 (m, 2H). Anal. ($C_{25}H_{21}N_3O_2S$) C, H, N.

(±)-6-Ethyl-6-[4-[(2-chloro-4-iodophenoxy)methyl]phenyl]-6,7-dihydrobenzo[*b*]pyrrolo[1,2-*d*][1,4]oxazepin-7-one (**4hh**). Compound **4hh** was obtained following the same procedure described for compound **4a** and using the appropriate phenol derivative. Purification was performed by means of flash chromatography (diethyl ether/petroleum ether 40–60 °C 1:5). Title compound was obtained as an amorphous white solid (48% yield): 1H NMR (300 MHz, $CDCl_3$) δ 1.04 (t, 3H, $J = 7.3$ Hz), 2.28–2.52 (m, 2H), 5.06 (s, 2H), 6.45–6.47 (m, 1H), 6.60 (d, 1H, $J = 8.5$ Hz), 6.96–7.44 (m, 11H), 7.67 (d, 1H, $J = 2.3$ Hz); ^{13}C NMR (75 MHz, $CDCl_3$) δ 8.6, 29.9, 32.4, 70.6, 77.4, 82.7, 95.9, 112.0, 116.1, 120.9, 121.9, 124.8, 125.5, 125.9, 126.2, 126.9, 127.2, 128.1, 134.0, 136.1, 136.7, 138.6, 146.8, 154.3, 192.8. Anal. ($C_{27}H_{21}ClINO_3$) C, H, N.

(±)-6-Ethyl-6-[4-[3-(2-hydroxy)ethylphenoxy)methyl]phenyl]-6,7-dihydrobenzo[*b*]pyrrolo[1,2-*d*][1,4]oxazepin-7-one (**4ii**). Compound **4ii** was obtained following the same procedure described for compound **4a** and using the appropriate phenol derivative (**12**). Purification was performed by means of flash chromatography (EtOAc). Title compound was obtained as an amorphous white solid (56% yield): 1H NMR (200 MHz, CD_3OD) δ 1.03 (t, 3H, $J = 7.0$ Hz), 2.40 (m, 2H), 2.54 (t, 2H, $J = 7.1$ Hz), 3.70 (t, 2H, $J = 7.1$ Hz), 4.95 (s, 2H), 6.47–6.51 (m, 1H), 6.63–6.79 (m, 3H), 6.93–7.46 (m, 11H); ESI-MS m/z $[M + H]^+$ 454 (100), $[M + Na]^+$ 476 $[M + K]^+$ 492. Anal. ($C_{29}H_{27}NO_4$) C, H, N.

3-(2-Bromoethyl)phenol (13). 3-(2-Hydroxyethyl)phenol (**12**) (1.0 g, 7.24 mmol) was dissolved in 40.0 mL of dry acetonitrile. Then triphenylphosphine (2.1 g, 7.96 mmol) and carbon tetrabromide (2.7 g, 7.96 mmol) were added. The reaction mixture was refluxed under argon atmosphere for 12 h. After cooling to room temperature, the reaction was quenched with 15% aqueous NaOH. The solvent was removed under reduced pressure, and the residue was extracted with EtOAc (3 × 100 mL). The organic layers were dried over sodium sulfate, filtered, and concentrated. The crude was purified by means of flash chromatography (EtOAc/*n*-hexane 2:1). Title compound was obtained as a colorless oil (55% yield). Spectroscopic data of title compound are consistent with those reported in the literature.⁴³

3-[2-(Diethylamino)ethyl]phenol (14). Bromide **13** (359 mg, 1.79 mmol) was dissolved in 15.0 mL of dry acetonitrile. To the refluxing solution, diethylamine (187 μ L, 1.79 mmol) and TEA (301 μ L, 2.15 mmol) were added, and the mixture was refluxed for 12 h. After the mix-

ture was cooled to room temperature, the solvent was removed under reduced pressure. The crude was purified by means of flash chromatography (MeOH/chloroform 1:9). Title compound was obtained as a yellow solid (71% yield). Spectroscopic data of title compound are consistent with those reported in the literature.⁴⁴

3-[2-(Pyrrolidin-1-yl)ethyl]phenol (15). Compound **15** was obtained following the same procedure described for compound **14** and using pyrrolidine. Purification was performed by means of flash chromatography (MeOH/chloroform 1:9). Title compound was obtained as a yellowish solid (60% yield). Spectroscopic data of title compound are consistent with those reported in the literature.⁴⁴

(±)-6-Ethyl-6-[4-[3-(2-diethylamino)ethylphenoxy)methyl]phenyl]-6,7-dihydrobenzo[*b*]pyrrolo[1,2-*d*][1,4]oxazepin-7-one (**4jj**). Compound **4jj** was obtained following the same procedure described for compound **4a** and using the appropriate phenol derivative (**14**). Purification was performed by means of flash chromatography (MeOH/chloroform 1:19). Title compound was obtained as an amorphous white solid (65% yield): 1H NMR (200 MHz, $CDCl_3$) δ 1.05 (t, 3H, $J = 6.8$ MHz), 1.22 (t, 6H, $J = 7.2$ Hz), 2.24–2.55 (m, 2H), 2.83–2.94 (m, 8H), 4.96 (s, 2H), 6.45 (m, 1H), 6.75–6.81 (m, 3H), 6.97–7.43 (m, 11H); ESI-MS m/z $[M + H]^+$ 509 (100). Anal. ($C_{33}H_{36}N_2O_3$) C, H, N.

(±)-6-Ethyl-6-[4-[3-(2-pyrrolidin-1-yl)ethylphenoxy)methyl]phenyl]-6,7-dihydrobenzo[*b*]pyrrolo[1,2-*d*][1,4]oxazepin-7-one (**4kk**). Compound **4kk** was obtained following the same procedure described for compound **4a** and using the appropriate phenol derivative (**15**). Purification was performed by means of flash chromatography (MeOH/chloroform 1:19). Title compound was obtained as an amorphous white solid (70% yield): 1H NMR (200 MHz, $CDCl_3$) δ 1.00 (t, 3H, $J = 6.9$ Hz), 1.59 (m, 4H), 2.24–2.29 (m, 2H), 2.41 (m, 4H), 2.65–2.69 (m, 4H), 4.91 (s, 2H), 6.39 (m, 1H), 6.74–7.36 (m, 14H); ESI-MS m/z $[M + H]^+$ 507 (100). Anal. ($C_{33}H_{34}N_2O_3$) C, H, N.

(±)-Ethyl 2-[4-[(Phenylthio)methyl]phenyl]-2-hydroxyacetate (**17a**). To a solution of thiophenol (103 μ L, 1.00 mmol) in dry THF (2.0 mL), sodium borohydride (18.0 mg, 0.460 mmol) was added. After the mixture was stirred for 30 min at room temperature, a solution of compound **16** (292 mg, 0.92 mmol) in 5.5 mL of dry THF was added dropwise. Then additional sodium borohydride (18.0 mg, 0.460 mmol) and sodium hydride (24 mg, 1.0 mmol) were added to the mixture. The mixture was allowed to stir for 12 h at 60 °C under argon atmosphere. After the mixture was cooled to room temperature, a saturated aqueous ammonium chloride solution was added. THF was removed under reduced pressure, and the residue was extracted with DCM (2 × 100 mL). The combined organic layers were dried over sodium sulfate, filtered, and concentrated. Purification was performed by means of flash chromatography (EtOAc/*n*-hexane 1:3). Pure title compound was obtained as an amorphous white solid (65% yield): 1H NMR (300 MHz, $CDCl_3$) δ 1.22 (t, 3H, $J = 7.0$ Hz), 3.45 (d, 1H, $J = 5.7$ Hz), 4.11–4.29 (m, 4H), 5.13 (d, 1H, $J = 5.7$ Hz), 7.18–7.40 (m, 9H); ESI-MS m/z $[M + Na]^+$ 325 $[M + K]^+$ 341 (100).

(±)-Ethyl 2-[4-[(2-Chlorophenylthio)methyl]phenyl]-2-hydroxyacetate (**17b**). Compound **17b** was obtained following the same procedure described for compound **17a** and using the appropriate thiophenol derivative. Purification was performed by means of flash chromatography (EtOAc/*n*-hexane 1:4). Title compound was obtained as an amorphous white solid (68% yield): 1H NMR (300 MHz, $CDCl_3$) δ 1.22 (t, 3H, $J = 7.0$ Hz), 3.44 (d, 1H, $J = 5.6$ Hz), 4.14–4.30 (m, 4H), 5.11 (d, 1H, $J = 5.6$ Hz), 7.07–7.40 (m, 8H); ESI-MS m/z $[M + H]^+$ 337 (100).

(±)-Ethyl 2-[4-[(3-Trifluoromethylphenylthio)methyl]phenyl]-2-hydroxyacetate (**17c**). Compound **17c** was obtained following the same procedure described for compound **17a** and using the appropriate thiophenol derivative. Purification was performed by means of flash chromatography (EtOAc/*n*-hexane 1:4). Title compound was obtained as an amorphous white solid (72% yield): 1H NMR (300 MHz,

CDCl_3) δ 1.22 (t, 3H, $J = 6.9$ Hz), 3.43 (d, 1H, $J = 5.6$ Hz), 4.08–4.32 (m, 4H), 5.10 (d, 1H, $J = 5.6$ Hz), 7.20–7.48 (m, 8H); ESI-MS m/z $[\text{M} + \text{H}]^+$ 371 (100).

(\pm)-Ethyl 2-Bromo-2-[4-[(phenylthio)methyl]phenyl]acetate (**18a**). To a solution of compound **17a** (243 mg, 0.880 mmol) in acetonitrile (10.0 mL), triphenylphosphine (232 mg, 0.880 mmol) and carbon tetrabromide (294 mg, 0.880 mmol) were added. After 2 h at room temperature, the mixture was stirred for 12 h at 50 °C. After the mixture was cooled to room temperature, a 5% NaOH aqueous solution was added. Acetonitrile was removed under reduced pressure, and the residue was extracted with EtOAc (3 \times 100 mL). The combined organic layers were dried over sodium sulfate, filtered, and concentrated. The crude product was purified by means of flash chromatography (EtOAc/*n*-hexane 1:6). Title compound was obtained as a pale yellow oil (51% yield): ^1H NMR (300 MHz, CDCl_3) δ 1.27 (t, 3H, $J = 6.9$ Hz), 4.10 (s, 2H), 4.23 (m, 2H), 5.31 (s, 1H), 7.19–7.29 (m, 6H), 7.47 (d, 2H, $J = 7.5$ Hz), 7.56 (m, 1H).

(\pm)-Ethyl 2-[4-[(2-Chlorophenylthio)methyl]phenyl]-2-bromoacetate (**18b**). Compound **18b** was obtained following the same procedure described for compound **18a**. Purification was performed by means of flash chromatography (EtOAc/*n*-hexane 1:6). Title compound was obtained as a pale yellow oil (59% yield): ^1H NMR (300 MHz, CDCl_3) δ 1.28 (m, 3H, $J = 7.1$ Hz), 4.13 (s, 2H), 4.21–4.29 (m, 2H), 5.31 (s, 1H), 7.13–7.49 (m, 8H).

(\pm)-Ethyl 2-[4-[(3-Trifluoromethylphenylthio)methyl]phenyl]-2-bromoacetate (**18c**). Compound **18c** was obtained following the same procedure described for compound **18a**. Purification was performed by means of flash chromatography (EtOAc/*n*-hexane 1:6). Title compound was obtained as a pale yellow oil (57% yield): ^1H NMR (300 MHz, CDCl_3) δ 1.27 (t, 3H, $J = 7.0$ Hz), 4.13 (s, 2H), 4.15–4.25 (m, 2H), 5.31 (s, 1H), 7.26–7.49 (m, 8H).

(\pm)-Ethyl 2-[2-(1*H*-Pyrrol-1-yl)phenoxy]-2-[4-[(phenylthio)methyl]phenyl]acetate (**19a**). To a solution of 2-(pyrrol-1-yl)-phenol²⁹ (80.0 mg, 0.500 mmol) in dry THF (4.0 mL), sodium hydride (14.0 mg, 0.560 mmol) was added. The mixture was stirred at room temperature for 30 min. Then compound **18a** (204.0 mg, 0.560 mmol) dissolved in 6.5 mL of dry THF was added dropwise, and the mixture was allowed to stir at 40 °C for 11 h. After the mixture was cooled, a saturated aqueous solution of ammonium chloride was added to the mixture. THF was removed under reduced pressure, and the residue was extracted with DCM (3 \times 60 mL). The combined organic layers were dried over sodium sulfate, filtered, and concentrated. The crude product was purified by means of flash chromatography (EtOAc/*n*-hexane 1:13). Title compound was obtained as a yellow oil (56% yield): ^1H NMR (300 MHz, CDCl_3) δ 1.16 (t, 3H, $J = 7.0$ Hz), 4.08–4.19 (m, 4H), 5.50 (s, 1H), 6.33 (m, 2H), 6.98–7.38 (m, 15H).

(\pm)-Ethyl 2-[2-(1*H*-Pyrrol-1-yl)phenoxy]-2-[4-[(2-chlorophenylthio)methyl]phenyl]acetate (**19b**). Compound **19b** was obtained following the same procedure described for compound **19a**. Purification was performed by means of flash chromatography (EtOAc/*n*-hexane 1:13). Title compound was obtained as a yellow oil (65% yield): ^1H NMR (300 MHz, CDCl_3) δ 1.17 (t, 3H, $J = 7.0$ Hz), 4.12–4.16 (m, 4H), 5.51 (s, 1H), 6.33 (m, 2H), 6.95–7.40 (m, 14H).

(\pm)-Ethyl 2-[2-(1*H*-Pyrrol-1-yl)phenoxy]-2-[4-[(3-trifluoromethylphenylthio)methyl]phenyl]acetate (**19c**). Compound **19c** was obtained following the same procedure described for compound **19a**. Purification was performed by means of flash chromatography (EtOAc/*n*-hexane 1:13). Title compound was obtained as a yellow oil (61% yield): ^1H NMR (300 MHz, CDCl_3) δ 1.16 (m, 3H, $J = 7.0$ Hz), 4.13–4.17 (m, 4H), 5.50 (s, 1H), 6.34 (m, 2H), 6.99–7.43 (m, 14H).

(\pm)-2-[2-(1*H*-Pyrrol-1-yl)phenoxy]-2-[4-[(phenylthio)methyl]phenyl]acetic Acid (**20a**). To a solution of compound **19a** (1.854 g, 4.180 mmol) in 50.0 mL of a THF/EtOH 1:1 mixture, a 5% aqueous

solution of NaOH (3.34 mL, 4.180 mmol) was added dropwise. The mixture was allowed to stir at room temperature for 12 h. Then the solvents were removed under reduced pressure and EtOAc was added. After the first extraction, the aqueous phase was treated with 6 N HCl until the acid precipitated. The aqueous phase was then extracted with EtOAc (3 \times 200 mL). The combined organic layers were dried over sodium sulfate, filtered, and concentrated. Title compound was obtained as an amorphous yellow solid and was used in the following step without further purification (99% yield): ^1H NMR (300 MHz, CDCl_3) δ 4.10 (s, 2H), 5.55 (s, 1H), 6.32 (m, 2H), 6.98–7.38 (m, 15H), 11.23 (br s, 1H).

(\pm)-2-[2-(1*H*-Pyrrol-1-yl)phenoxy]-2-[4-[(2-chlorophenylthio)methyl]phenyl]acetic Acid (**20b**). Compound **20b** was obtained following the same procedure described for **20a**. Title compound was obtained as an amorphous yellow solid and was used in the following step without further purification (98% yield): ^1H NMR (300 MHz, CDCl_3) δ 4.11 (s, 2H), 5.56 (s, 1H), 6.33 (m, 2H), 6.95–7.40 (m, 14H), 9.56 (br s, 1H).

(\pm)-2-[2-(1*H*-Pyrrol-1-yl)phenoxy]-2-[4-[(3-trifluoromethylphenylthio)methyl]phenyl]acetic Acid (**20c**). Compound **20c** was obtained following the same procedure described for **20a**. Title compound was obtained as an amorphous yellow solid and was used in the following step without further purification (99% yield): ^1H NMR (300 MHz, CDCl_3) δ 4.10 (s, 2H), 5.55 (s, 1H), 6.32 (m, 2H), 6.98–7.41 (m, 14H), 9.73 (br s, 1H).

(\pm)-6-[4-[(Phenylthio)methyl]phenyl]-6,7-dihydrobenzo[*b*]pyrrolo[1,2-*d*][1,4]oxazepin-7-one (**4II**). To a refluxing solution of **20a** (1.620 g, 3.900 mmol) in dry DCM (40.0 mL), PCl_5 (894 mg, 4.290 mmol) was added. The resulting mixture was stirred under reflux for 7 h. After the mixture was cooled to room temperature, a saturated aqueous solution of sodium bicarbonate was added. The residue was extracted with DCM (3 \times 100 mL). The combined organic layers were dried over sodium sulfate, filtered, and concentrated. The crude was purified by means of flash chromatography (EtOAc/*n*-hexane 1:9). Title compound was obtained as an amorphous white solid (80% yield): ^1H NMR (300 MHz, CDCl_3) δ 4.08 (s, 2H), 5.54 (s, 1H), 6.51 (m, 1H), 7.11–7.42 (m, 15H). Anal. ($\text{C}_{25}\text{H}_{19}\text{NO}_2\text{S}$) C, H, N.

(\pm)-6-[4-[(2-Chlorophenylthio)methyl]phenyl]-6,7-dihydrobenzo[*b*]pyrrolo[1,2-*d*][1,4]oxazepin-7-one (**4mm**). Compound **4mm** was obtained following the same procedure described for **4II**. The crude product was purified by means of flash chromatography (EtOAc/*n*-hexane 1:9). Title compound was obtained as an amorphous white solid (69% yield): ^1H NMR (300 MHz, CDCl_3) δ 4.13 (s, 2H), 5.52 (s, 1H), 6.51 (m, 1H), 7.06–7.42 (m, 14H). Anal. ($\text{C}_{25}\text{H}_{18}\text{ClNO}_2\text{S}$) C, H, N.

(\pm)-6-[4-[(3-Trifluoromethylphenylthio)methyl]phenyl]-6,7-dihydrobenzo[*b*]pyrrolo[1,2-*d*][1,4]oxazepin-7-one (**4nn**). Compound **4nn** was obtained following the same procedure described for **4II**. The crude product was purified by means of flash chromatography (EtOAc/*n*-hexane 1:9). Title compound was obtained as an amorphous white solid (55% yield): ^1H NMR (300 MHz, CDCl_3) δ 4.10 (s, 2H), 5.53 (s, 1H), 6.52 (m, 1H), 7.08–7.45 (m, 14H). Anal. ($\text{C}_{26}\text{H}_{18}\text{F}_3\text{NO}_2\text{S}$) C, H, N.

(\pm)- α -[[2-(1*H*-Pyrrol-1-yl)phenyl]thio]-*p*-tolylacetic Acid Ethyl Ester (**22**). A suspension of **21** (2.50 g, 11.43 mmol) in absolute EtOH (45.0 mL) was heated to reflux. Sodium borohydride (550 mg, 14.50 mmol) was then added in portions over 30 min. Then the mixture was allowed to cool to room temperature and (\pm)- α -bromo-*p*-tolylacetic acid ethyl ester (4.0 g, 15.80 mmol) in 20.0 mL of absolute EtOH was added dropwise. After 8 h water was added to the mixture, and EtOH was removed under reduced pressure. The residue was extracted with chloroform (3 \times 150 mL). The combined organic layers were dried over sodium sulfate, filtered, and concentrated. The crude was purified by means of flash chromatography (chloroform/*n*-hexane 1:1). Title compound was obtained as an amorphous white solid (79% yield): ^1H NMR (300 MHz, CDCl_3) δ 1.13 (t, 3H, $J = 7.1$ Hz), 2.35 (s, 3H), 4.09

(m, 2H), 4.43 (s, 1H), 6.43 (t, 2H, $J = 1.8$ Hz), 7.01 (t, 2H, $J = 1.9$ Hz), 7.14 (d, 2H, $J = 7.2$ Hz), 7.28–7.39 (m, 5H), 7.61 (d, 1H, $J = 7.3$ Hz).

(±)- α -[2-(1H-Pyrrol-1-yl)phenyl]thio-*p*-tolylacetic Acid (23). Compound 23 was obtained following the same procedure described 20a. Title compound was obtained as a yellowish amorphous solid and was used in the following step without further purification (99% yield): ^1H NMR (300 MHz, CDCl_3) δ 2.26 (s, 3H), 4.36 (s, 1H), 6.39 (t, 2H, $J = 1.8$ Hz) 7.00–7.58 (m, 10 H), 9.69 (br s, 1H).

(±)-6-(*p*-Tolyl)pyrrolo[2,1-*d*][1,5]benzothiazepin-7-(6H)-one (24). Compound 24 was obtained following the same procedure described for 4II. The crude product was purified by means of flash chromatography (EtOAc/*n*-hexane 1:7). Title compound was obtained as an amorphous white solid (65% yield): ^1H NMR (300 MHz, CDCl_3) δ 2.25 (s, 3H), 4.79 (s, 1H), 6.52 (m, 1H), 6.95–7.46 (m, 10H).

(±)-6-Ethyl-6-(*p*-tolyl)pyrrolo[2,1-*d*][1,5]benzothiazepin-7-(6H)-one (25). A solution of 24 (150 mg, 0.490 mmol) in dry THF (5.0 mL) was added dropwise to a suspension of potassium hydride (35% in mineral oil, 63 mg, 0.540 mmol) in dry THF (1.5 mL). The mixture was stirred for 2 h at room temperature. Then iodoethane (223 μL , 2.760 mmol) was slowly added and the mixture was allowed to stir at room temperature for 15 h. After that time a saturated aqueous solution of ammonium chloride was added and THF was removed under reduced pressure and the residue was extracted with DCM (3×100 mL). The combined organic layers were dried over sodium sulfate, filtered, and concentrated. The product was purified by means of flash chromatography (DCM/petroleum ether 40–60 °C 1:1). Pure title compound was obtained as an amorphous white solid (70% yield): ^1H NMR (300 MHz, CDCl_3) δ 1.06 (t, 3H, $J = 7.3$ Hz), 2.15–2.29 (m, 4H), 2.42–2.59 (m, 1H), 6.41 (m, 1H), 6.81–7.42 (m, 10H).

(±)-6-Ethyl-6-(4-bromomethylphenyl)pyrrolo[2,1-*d*][1,5]benzothiazepin-7(6H)-one (26). To a solution of 25 (100 mg, 0.300 mmol) in carbon tetrachloride (8.5 mL), *N*-bromosuccinimide (59 mg, 0.330 mmol) and a catalytic amount of AIBN were added. The mixture was stirred for 2.5 h under reflux. After the mixture was cooled to room temperature, succinimide was removed by filtration and the solvent was evaporated under reduced pressure. The residue was taken up with DCM, and the solution was washed with brine. The organic layer was dried over sodium sulfate, filtered, and concentrated. The product was purified by means of flash chromatography (EtOAc/*n*-hexane 1:7). Title compound was obtained as an amorphous white solid (85% yield): ^1H NMR (300 MHz, CDCl_3) δ 1.08 (t, 3H, $J = 7.4$ Hz), 2.11–2.30 (m, 1H), 2.44–2.63 (m, 1H), 4.28 (s, 2H), 6.44 (m, 1H), 6.97–7.48 (m, 10H).

(±)-6-Ethyl-6-[4-[(2-chlorophenylthio)methyl]phenyl]-6,7-dihydrobenzo[*b*]pyrrolo[1,2-*d*][1,4]thiazepin-7-one (4oo). Compound 4oo was obtained following the same procedure described for compound 4a. Purification was performed by means of flash chromatography (EtOAc/*n*-hexane 1:10). Title compound was obtained as an amorphous white solid (82% yield): ^1H NMR (300 MHz, CDCl_3) δ 1.07 (t, 3H, $J = 7.2$ Hz), 2.18–2.28 (m, 1H), 2.47–2.56 (m, 1H), 3.95 (s, 2H), 6.44 (m, 1H), 6.94–7.17 (m, 12H), 7.33–7.35 (m, 1H), 7.41–7.46 (m, 1H). Anal. ($\text{C}_{27}\text{H}_{22}\text{ClNOS}_2$) C, H, N.

(±)-6-Ethyl-6-[4-[(4-iodophenylthio)methyl]phenyl]-6,7-dihydrobenzo[*b*]pyrrolo[1,2-*d*][1,4]thiazepin-7-one (4pp). Compound 4pp was obtained following the same procedure described for compound 4a. Purification was performed by means of flash chromatography (petroleum ether 40–60 °C/diethyl ether 5:1). Title compound was obtained as an amorphous white solid (70% yield): ^1H NMR (300 MHz, CDCl_3) δ 1.07 (t, 3H, $J = 7.0$ Hz), 2.04–2.27 (m, 1H), 2.47–2.57 (m, 1H), 3.88 (s, 2H), 6.43–6.45 (m, 1H), 6.85–7.19 (m, 10H), 7.33–7.35 (m, 1H), 7.45–7.52 (m, 3H); ^{13}C NMR (75 MHz, CDCl_3) δ 10.4, 34.1, 38.2, 68.7, 91.3, 111.2, 122.2, 124.0, 126.2, 126.6, 128.1, 128.1, 128.5, 128.9, 131.4, 135.5, 135.9, 136.4, 136.5, 137.9, 139.1, 142.04, 189.4. Anal. ($\text{C}_{27}\text{H}_{22}\text{INOS}_2$) C, H, N.

(±)-6-Ethyl-6-[4-[[4-[2-(trimethylsilyl)ethynyl]phenylthio]methyl]phenyl]-6,7-dihydrobenzo[*b*]pyrrolo[1,2-*d*][1,4]thiazepin-7-one (4qq). Compound 4qq was obtained following the same procedure described for compound 4p. Purification was performed by means of flash chromatography (EtOAc/*n*-hexane 1:8). Title compound was obtained as an amorphous white solid (80% yield): ^1H NMR (300 MHz, CDCl_3) δ 0.24 (s, 9H), 1.07 (t, 3H, $J = 7.3$ Hz), 2.17–2.24 (m, 1H), 2.50–2.55 (m, 1H), 3.91 (s, 2H), 6.42–6.45 (m, 1H), 6.93–7.34 (m, 13H), 7.46–7.48 (m, 1H); ^{13}C NMR (75 MHz, CDCl_3) δ 0.2, 10.3, 34.1, 37.9, 68.7, 95.0, 104.9, 111.2, 120.9, 122.1, 124.0, 126.2, 126.6, 128.0, 128.5, 128.8, 128.9, 129.9, 132.3 (2C), 135.5, 135.9, 136.5, 137.4, 139.1, 142.0. Anal. ($\text{C}_{32}\text{H}_{31}\text{NOS}_2\text{Si}$) C, H, N.

Construction of Recombinant Bacterial Expression Vector for *hAK*. An amount of 1 μg of total RNA extracted from HeLaS-3 cells using the Rneasy Mini kit (Quiagen) was retrotranscribed by using RT-PCR method. cDNA of *hAK* was then amplified by using the following specific primers: 5'-GGAGGGCGGATCCATGACGT CAGTCAGAG-3' (primer 1, sense) and 5'-GTGTTTAAAGCTTTTCCATCAGTGAAGTC-3' (primer 2, antisense), presenting the *NheI* and *HindIII* restriction sites, respectively. The amplified region (1070 bp long) containing the complete *hAK* coding sequence was inserted into the multiple cloning site of pTrcHisA (Invitrogen). His-tagged *hAK* sequence encodes for the complete 345 amino acids enzyme containing a 6-His tag at its NH_2 terminus.

Expression and Purification of Recombinant *hAK* from Bacterial Cells. Expression and purification of the *hAK* were carried out as described by the manufacturer of the Ni-NTA Superflow resin (Quiagen). Briefly, a fresh overnight saturated culture of *E. coli* (DH5 α strain) transformed with pHis-*hAK* was diluted 1:100 in 1 L of 2XYT broth containing ampicillin (60 $\mu\text{g}/\text{mL}$) and incubated at 25 °C with shaking. At 0.6 OD₆₀₀ IPTG was added to a final concentration of 0.4 mM, and the culture was incubated for a further 2 h at 37 °C. The bacterial cells pellet was resuspended in four volumes of lysis buffer (50 mM sodium phosphate, pH 8.0, 300 mM NaCl, 10 mM imidazole, 1 mM phenylmethylsulfonyl fluoride, and 1 mg/mL lysozyme) and incubated on ice for 30 min. Cells were then homogenized and sonicated on ice, and the lysate was centrifuged at 10000g for 30 min at 4 °C. The supernatant was loaded onto a Ni-NTA Superflow column (1 mL). The column was then washed at a flow rate of 0.25 mL/min with lysis buffer and then with 50 mM sodium phosphate buffer, pH 8.0, containing 300 mM NaCl and 20 mM imidazole. The protein was then step-eluted with 250 mM imidazole in 50 mM sodium phosphate buffer, pH 8.0, and 300 mM NaCl. Fractions were collected for enzymatic activity analysis. The enzyme, collected from peak fractions, was dialyzed against 50 mM Tris-HCl, pH 7.5, 1 mM 1,4-dithiothreitol (DTT) and then frozen in liquid nitrogen until used.

Adenosine Kinase Assays. *hAK* was assayed with a radiochemical method which measures the formation of [^3H]AMP from [^3H]Ado. The enzyme was incubated at 37 °C in 25 μL of a mixture containing 32 mM Tris-HCl (pH 7.5), 20 mM KCl, 0.1 mM MgCl_2 , 1 mM ATP, and 0.5 μM [^3H]Ado (2200 cpm/pmol). The reaction was terminated by spotting 20 μL of the incubation mixture on a 25 mm diethylaminoethyl paper disk (DE-81 paper; Whatman). The disk was washed twice in an excess of 1 mM ammonium formate, pH 3.6, in order to remove unconverted nucleoside, once in distilled water, and finally in ethanol. Radioactive AMP was estimated by scintillation counting in 1 mL of BetaMax scintillating fluid (ICN Pharmaceutical). One unit (U) is defined as the amount of enzyme catalyzing the formation of 1 nmol of AMP in 1 h at 37 °C.

In inhibition studies, increasing concentrations of each compound were tested in duplicate in two independent assays, as described above. Stock solutions of compounds, in 100% DMSO, were diluted in water to a final DMSO concentration of 1%. Controls without inhibitor were also incubated in the presence of 1% DMSO.

In Vitro Ado Phosphorylation. When *hAK* activity was determined in vitro, HeLaS-3 cells were grown in Dulbecco's modified Eagle medium (DMEM) with fetal calf serum at 37 °C. After trypsinization, they were resuspended in DMEM without calf serum at 10^6 cells/mL (100 μ L) and incubated at 37 °C in the presence of 0, 10, or 50 μ M **4a** and 3 μ Ci of [3 H]Ado (25 Ci/mmol). At times 0, 10, 20, 30, and 40 min, 80 μ L samples of culture were spotted on 25 mm DE-81 (Whatman) filters, washed, and counted as above-described.

Assay of *hAK* Activity in HeLaS-3 Crude Extract. HeLaS-3 cells (2.5×10^6), grown in DMEM, were washed in phosphate buffered saline (PBS), centrifuged (1000g), and resuspended in 10 mM Hepes, pH 7.3, 1 mM DTT, and 0.5 mM PMSF. After 30 min on ice, cells were disrupted by dounce homogenization and centrifuged 20 min at 10000g. Supernatant (protein concentration of 6.0 mg/mL) was used as HeLa crude extract. In *hAK* assay, as described above, 2 μ L of HeLaS-3 crude extract replaced recombinant *hAK*.

In Vitro Incorporation of [3 H]Thymidine and [3 H]Uridine. HeLaS-3 cells were grown in DMEM with fetal calf serum at 37 °C. After trypsinization, they were resuspended in DMEM without calf serum at 10^6 cells/mL (100 μ L) and incubated at 37 °C in the presence of 0, 10, or 50 μ M **4a** (or ddCyd) and 5 μ Ci of either [3 H]thymidine (25 Ci/mmol) or [3 H]uridine (22 Ci/mmol). At times 0, 10, 20, 30, and 40 min, 80 μ L samples of culture were spotted on 25 mm GF/C (Whatman) filters which were then washed three times (10 min) in 5% trichloroacetic acid, twice in ethanol and dried. Remaining radioactivity was measured as described above.

Measurement of Cell Viability: Dye Exclusion Assay. Chronic myeloid leukemia cells, from K562 cell line grown in Roswell Park Memorial Institute (RPMI) 1640 medium containing 10% fetal calf serum, were seeded in a 96-well microplate at 5000 cells/mL (150 μ L/well). After 15 h at 37 °C in 5% CO₂, an amount of 50 μ L/well of serial dilutions of the compound to test was added. The microplate, sealed with Saran wrap to limit evaporation of the medium and diffusion of metabolic carbon dioxide, was then incubated for 7 days in the above conditions. Then an amount of 50 μ L of the cell suspension was removed from the well and mixed with 50 μ L of trypan blue solution (0.5% in PBS). Both viable cells (not stained) and dead cells (blue stained) were then counted on a Bürker cell counter. Each point was done in triplicate, and the number of cells counted in each well is the average of four determinations.

Measurement of Cell Growth. HeLaS-3 and Cen3tel cells (8×10^4) were incubated in multiwell plates at 37 °C in 2 mL of DMEM supplemented with 10% fetal calf serum, 5 mM L-glutamine, and 50 μ g/mL Gentamycin. Cells were left in the presence or in absence (control) of 40 μ M **4a** for 3 days (medium and compound were replaced every day). Sample of the cultures were counted every day. In order to evaluate the capability of the cells to recover from the cytostatic effect of the compound, cells were washed and left growing for 2 days and then counted. Cell counting was performed after trypsinization.

Analysis of Possible **4a Intracellular Degradation.** **4a** (1 mM) was incubated at 37 °C for 0, 1, 5, and 20 h in 175 μ L of HeLaS-3 crude extract, prepared as described above. After incubation, samples were frozen and lyophilized. In each tube, 50 μ L of cold (−20 °C) MeOH was added. The mixtures were then vortexed for 10 min and centrifuged at 10000g for 15 min. Supernatants were transferred into new tubes. MeOH extraction was repeated on each pellet. The two supernatants of each incubation time were combined, lyophilized, and resuspended in 25 μ L of 5% DMSO. An amount of 20 μ L of these solutions was analyzed by reverse phase HPLC, as previously described,⁴⁵ in order to evaluate the total amount of **4a** present in the samples.

Cytotoxicity Assay. The cytotoxicity of the different compounds was evaluated using the murine fibroblast cell line (3T3 cells). Cell proliferation was analyzed by the 3-(4,5-dimethylthiazol-2-yl)-2,5-diphenyltetrazolium bromide assay. The data processing included the Student's *t* test with *p* < 0.05 taken as significance level.

Measurement of Viability in HL-60 Cells. Human promyelocytic leukemia HL-60 cells were obtained from the ECACC. Cells were maintained in RPMI-1640 medium enhanced with GlutaMAX-I and supplemented with 10% fetal bovine serum, 50 units/mL penicillin, and 50 μ g/mL streptomycin (all from Gibco, Invitrogen, Carlsbad, CA, U.S.). Cells were maintained in a humidified incubator at 37 °C in 5% CO₂.

Cell proliferation was monitored using AmalarBlue dye (BioSource, Invitrogen, Carlsbad, CA, U.S.) which changes to a fluorescent state in the reduced environment of living cells. Cells (40 000 cells/well) were seeded on 96-well plates for 24 h and then treated with vehicle (0.1% (v/v) DMSO) or a range of concentrations of **4a** compound for 72 h. AmalarBlue (final concentration 10% (v/v)) was added and incubated for a further 4.5 h at 37 °C. Fluorescence was measured at an excitation wavelength of 544 nm and an emission wavelength of 590 nm using a SpectraMax Gemini spectrofluorometric plate reader (Molecular Devices, Sunnyvale, CA). The results were expressed as the percentage cell viability relative to vehicle-treated control cells (100%). Dose-response curves were plotted, and IC₅₀ values (concentration of drug resulting in 50% reduction in cell viability) were obtained using Prism GraphPad 4.

Determination of Apoptosis in HL-60 Cells. Following treatment with vehicle (0.1% DMSO) or a range of concentrations of **4a** for 24, 48, or 78 h, cells were harvested by centrifugation at 800g for 10 min. Cell pellets were resuspended in 200 μ L of PBS and fixed by a dropwise addition of 2 mL of ice-cold 70% (v/v) ethanol/PBS while gently vortexing. Following overnight fixation at −20 °C the cells were again centrifuged to remove the ethanol and resuspended in PBS supplemented with 0.5 mg/mL RNase A and 0.15 mg/mL propidium iodide (PI). Cells were incubated in the dark at 37 °C for 30 min. The PI fluorescence was measured on a linear scale using a FACS Calibur flow cytometer (Becton Dickinson, San Jose, CA, U.S.). Data collections (10 000 events per sample) were gated to exclude cell debris and cell aggregates. PI fluorescence was proportional to the amount of DNA present in each entity and therefore indicated the stage of the cell cycle. Cells in G₀/G₁ were diploid (2N DNA content). Cells in the S phase had DNA contents between 2N and 4N. Cells in G₂/M were tetraploid (4N DNA content), while apoptotic cells were hypoploid and contained <2N DNA (pre-G₁). Polyploid cells had a DNA content of >4N. All data were recorded and analyzed using the CellQuest software (Becton Dickinson, San Jose, CA, U.S.). Statistical analysis was performed using Prism GraphPad 4. *P* values were obtained using two-tailed paired student's *t* tests. *P* < 0.05 was considered significant.

Adenosine Deaminase Enzymatic Assay⁴⁶. ADA type IX from bovine spleen (150–200 U/mg) and Ado were purchased from Sigma Chemical Co. All other chemicals were of reagent grade. The activity of ADA was determined spectrophotometrically by monitoring for 2 min the change in absorbance at 262 nm, which is due to the deamination of Ado catalyzed by the enzyme. The change in Ado concentration/min was determined using a Beckman DU-64 kinetics software program (Solf Pack TM module). ADA activity was assayed at 30 °C in a reaction mixture containing 50 μ M Ado, 50 mM potassium phosphate buffer, pH 7.2, and 0.3 nM enzyme solution in a total volume of 500 μ L. The inhibitory activity of the newly synthesized compounds was assayed by adding 100 μ L of the inhibitor solution to the reaction mixture described above. All the inhibitors were dissolved in water, and the solubility was facilitated by using DMSO, whose concentration never exceeded 4% in the final reaction mixture. To correct for the non-enzymatic change in Ado concentration and the absorption by the test compounds, a reference blank containing all of the above assay components except the substrate was prepared. The inhibitory effect of the new derivatives was routinely estimated at 100 μ M. Results are expressed as the mean \pm SEM of percentage inhibition values, obtained through two determinations carried out in triplicate.

Molecular Modeling. Ligand Binding Site Prediction. Two programs were used for the ligand binding site prediction: QSiteFinder

(<http://www.bioinformatics.leeds.ac.uk/qsitefinder>) and SiteMap from Schrödinger. The first is a server for ligand binding site prediction and works by binding hydrophobic (CH_3) probes to the protein and finding clusters of probes with the most favorable binding energy. These clusters are placed in rank order of the likelihood of being a binding site according to the sum total binding energies for each cluster. The programs were both used on either the closed (PDB code 1BX4) or the open (PDB code 2I6B) enzyme conformation as retrieved from the Protein Data Bank and produced comparable results.

Docking Simulations. The Autodock program (version 4.0)⁴⁷ was used just for the blind docking, although it has previously demonstrated to be successful also in the prediction of enzyme inhibitors binding modes.^{48–50} The inhibitor structure of **4a** (S and R enantiomers) were first generated through the Dundee PRODRG2 Server (<http://davapc1.bioch.dundee.ac.uk/prodrg>). For the protein setup, to create initial coordinates for docking studies, all water molecules of the crystal structures were removed and excluded from calculations while the two cocrystallized Ado were retained accordingly with the noncompetitive behavior of **4a** with regard to adenosine and/or ATP. The docking area has been defined by a box large enough to comprise the entire protein and centered on Ser 65 C α . Grids points of $126 \times 126 \times 126$ with 0.531 Å spacing were calculated around the docking area for all the ligand atom types using AutoGrid4. One-hundred separate docking calculations were performed. Each docking calculation consisted of 25×10^6 energy evaluations using the Lamarckian genetic algorithm local search (GALS) method. A low-frequency local search according to the method of Solis and Wets was applied to docking trials to ensure that the final solution represents a local minimum. Each docking run was performed with a population size of 150, and 300 rounds of Solis and Wets local search were applied with a probability of 0.06. A mutation rate of 0.02 and a crossover rate of 0.8 were used to generate new docking trials for subsequent generations. The docking results from each of the 100 calculations were clustered on the basis of root-mean square deviation (rmsd = 2.0 Å) between the Cartesian coordinates of the ligand atoms and were ranked on the basis of the free energy of binding. The pocket detected as putative allosteric binding site by the Autodock program was further investigated with a subsequent “focused” docking step in order to characterize the **4a** and its derivatives binding modes. The “focused” docking was performed with the aid of Glide software.⁵¹ The latter was preferred over the Autodock, as all our derivatives can exist in two different stereoisomers (one chiral carbon) and two different conformations (flipping of the pyrrolobenzoxa(thia)zepinone scaffold) and, different from Autodock, Glide is able to generate all these variations for each derivative and analyze all of them in a single docking run. The inhibitor structures were first generated through the Dundee PRODRG2 server. Then geometry optimized ligands were prepared using Lig-Prep 2.3 as implemented in Maestro. The target protein was prepared through the Protein Preparation Wizard of the graphical user interface Maestro and the OPLS-2001 force field. Water molecules were removed. Hydrogen atoms were added, and minimization was performed until the rmsd of all heavy atoms was within 0.3 Å of the crystallographically determined positions. The binding pocket was identified by placing a 15 Å cube centered on the mass center of the best ranked pose of **4a**, obtained from AutoDock4 blind docking. Molecular docking calculations were performed with the aid of Glide 5.5 in standard precision (SP) mode, using Glidescore for ligand ranking. For multiple ligand docking experiments, an output maximum of 5000 ligand poses per docking run with a limit of 100 poses for each ligand was adopted.

■ ASSOCIATED CONTENT

S Supporting Information. SDS–PAGE results (Figure 1) and elemental analyses for final compounds. This material is available free of charge via the Internet at <http://pubs.acs.org>.

■ AUTHOR INFORMATION

Corresponding Author

*Phone: 0039-0577-234172. Fax: 0039-0577-234333. E-mail: campiani@unisi.it.

■ ACKNOWLEDGMENT

This work was partially supported by FIRB Grant RBAU01LSR4_001 (to F.F.).

■ ABBREVIATIONS USED

AK, adenosine kinase; Ado, adenosine; AMP, adenosine monophosphate; CNS, central nervous system; PNS, peripheral nervous systems; hAK, human adenosine kinase; HL, human leukemia; NNhAKIs, non-nucleoside human adenosine kinase inhibitors; SAR, structure–activity relationship; THF, tetrahydrofuran; TEA, triethylamine; DABCO, 1,4-diazabicyclo[2.2.2]octane; DMF, dimethylformamide; DCM, dichloromethane; AIBN, 2,2'-azodiisobutyronitrile; HeLaS-3, human epithelial carcinoma cell line subclone S3; EWG, electron-withdrawing group; EDG, electron-donating group; ddCyd, 2',3'-dideoxycytidine; DMSO, dimethylsulfoxide; ADA, adenosine deaminase; IPTG, isopropylthio- β -D-galactoside; DTT, 1,4-dithiothreitol; DMEM, Dulbecco's modified Eagle medium; PBS, phosphate buffered saline; RPMI, Roswell Park Memorial Institute; PI, propidium iodide

■ REFERENCES

- (1) Maj, M.; Singh, B.; Gupta, R. S. The influence of inorganic phosphate on the activity of adenosine kinase. *Biochim. Biophys. Acta* **2000**, *1476*, 33–42.
- (2) Chang, C. H.; Cha, S.; Brockman, R. W.; Bennett, L. L., Jr. Kinetic studies of adenosine kinase from L1210 cells: a model enzyme with a two-site ping-pong mechanism. *Biochemistry* **1983**, *22*, 600–611.
- (3) Hawkins, C. F.; Bagnara, A. S. Adenosine kinase from human erythrocytes: kinetic studies and characterization of adenosine binding sites. *Biochemistry* **1987**, *26*, 1982–1987.
- (4) Lin, B. B.; Hurley, M. C.; Fox, I. H. Regulation of adenosine kinase by adenosine analogs. *Mol. Pharmacol.* **1988**, *34*, 501–505.
- (5) Mathews, I. I.; Erion, M. D.; Ealick, S. E. Structure of human adenosine kinase at 1.5 Å resolution. *Biochemistry* **1998**, *37*, 15607–15620.
- (6) Borowiec, A.; Lechward, K.; Tkacz-Stachowska, K.; Skladanowski, A. C. Adenosine as a metabolic regulator of tissue function: production of adenosine by cytoplasmic 5'-nucleotidases. *Acta Biochim. Pol.* **2006**, *53*, 269–278.
- (7) Boison, D.; Chen, J. F.; Fredholm, B. B. Adenosine signaling and function in glial cells. *Cell Death Differ.* **2010**, *17*, 1071–1082.
- (8) Ralevic, V.; Burnstock, G. Receptors for purines and pyrimidines. *Pharmacol. Rev.* **1998**, *50*, 413–492.
- (9) Latini, S.; Pedata, F. Adenosine in the central nervous system: release mechanisms and extracellular concentrations. *J. Neurochem.* **2001**, *79*, 463–484.
- (10) Hasko, G.; Cronstein, B. N. Adenosine: an endogenous regulator of innate immunity. *Trends Immunol.* **2004**, *25*, 33–39.
- (11) Kowaluk, E. A.; Jarvis, M. F. Therapeutic potential of adenosine kinase inhibitors. *Expert Opin. Invest. Drugs* **2000**, *9*, 551–564.
- (12) Boison, D. Adenosine kinase, epilepsy and stroke: mechanisms and therapies. *Trends Pharmacol. Sci.* **2006**, *27*, 652–658.
- (13) Yang, D.; Yaguchi, T.; Yamamoto, H.; Nishizaki, T. Intracellularly transported adenosine induces apoptosis in HuH-7 human hepatoma cells by downregulating c-FLIP expression causing caspase-3/-8 activation. *Biochem. Pharmacol.* **2007**, *73*, 1665–1675.
- (14) Saitoh, M.; Nagai, K.; Nakagawa, K.; Yamamura, T.; Yamamoto, S.; Nishizaki, T. Adenosine induces apoptosis in the human gastric

cancer cells via an intrinsic pathway relevant to activation of AMP-activated protein kinase. *Biochem. Pharmacol.* **2004**, *67*, 2005–2011.

(15) Barry, C. P.; Lind, S. E. Adenosine-mediated killing of cultured epithelial cancer cells. *Cancer Res.* **2000**, *60*, 1887–1894.

(16) Gomtsyan, A.; Lee, C. H. Nonnucleoside inhibitors of adenosine kinase. *Curr. Pharm. Des.* **2004**, *10*, 1093–1103.

(17) Gomtsyan, A.; Didomenico, S.; Lee, C. H.; Matulenko, M. A.; Kim, K.; Kowaluk, E. A.; Wismer, C. T.; Mikusa, J.; Yu, H.; Kohlhaas, K.; Jarvis, M. F.; Bhagwat, S. S. Design, synthesis, and structure–activity relationship of 6-alkynylpyrimidines as potent adenosine kinase inhibitors. *J. Med. Chem.* **2002**, *45*, 3639–3648.

(18) Jacobson, K. A.; Hoffmann, C.; Cattabeni, F.; Abbracchio, M. P. Adenosine-induced cell death: evidence for receptor-mediated signaling. *Apoptosis* **1999**, *4*, 197–211.

(19) Mlejnek, P.; Dolezel, P. Apoptosis induced by N6-substituted derivatives of adenosine is related to intracellular accumulation of corresponding mononucleotides in HL-60 cells. *Toxicol. in Vitro* **2005**, *19*, 985–990.

(20) Tanaka, Y.; Yoshihara, K.; Tsuyuki, M.; Kamiya, T. Apoptosis induced by adenosine in human leukemia HL-60 cells. *Exp. Cell Res.* **1994**, *213*, 242–252.

(21) Mc Gee, M. M.; Gemma, S.; Butini, S.; Ramunno, A.; Zisterer, D. M.; Fattorusso, C.; Catalanotti, B.; Kukreja, G.; Fiorini, I.; Pisano, C.; Cucco, C.; Novellino, E.; Nacci, V.; Williams, D. C.; Campiani, G. Pyrrolo[1,5]benzoxa(thia)zepines as a new class of potent apoptotic agents. Biological studies and identification of an intracellular location of their drug target. *J. Med. Chem.* **2005**, *48*, 4367–4377.

(22) McGaraughty, S.; Cowart, M.; Jarvis, M. F.; Berman, R. F. Anticonvulsant and antinociceptive actions of novel adenosine kinase inhibitors. *Curr. Top. Med. Chem.* **2005**, *5*, 43–58.

(23) Park, J.; Vaidyanathan, G.; Singh, B.; Gupta, R. S. Identification and biochemical studies on novel non-nucleoside inhibitors of the enzyme adenosine kinase. *Protein J.* **2007**, *26*, 203–212.

(24) Fattorusso, C.; Gemma, S.; Butini, S.; Huleatt, P.; Catalanotti, B.; Persico, M.; De Angelis, M.; Fiorini, I.; Nacci, V.; Ramunno, A.; Rodriguez, M.; Greco, G.; Novellino, E.; Bergamini, A.; Marini, S.; Coletta, M.; Maga, G.; Spadari, S.; Campiani, G. Specific targeting highly conserved residues in the HIV-1 reverse transcriptase primer grip region. Design, synthesis, and biological evaluation of novel, potent, and broad spectrum NNRTIs with antiviral activity. *J. Med. Chem.* **2005**, *48*, 7153–7165.

(25) Springer, D. M.; Luh, B. Y.; Goodrich, J.; Bronson, J. J. Anti-MRSA cepheps. Part 2: C-7 cinnamic acid derivatives. *Bioorg. Med. Chem.* **2003**, *11*, 265–279.

(26) Barnish, I. T.; Cross, P. E.; Danilewicz, J. C.; Dickinson, R. P.; Stopher, D. A. Promotion of carbohydrate oxidation in the heart by some phenylglyoxylic acids. *J. Med. Chem.* **1981**, *24*, 399–404.

(27) Fiorini, I.; Nacci, V.; Ciani, S. M.; Garofalo, A.; Campiani, G.; Savini, L.; Novellino, E.; Greco, G.; Bernasconi, P.; Mennini, T. Novel ligands specific for mitochondrial benzodiazepine receptors: 6-arylpyrrolo[2,1-*d*][1,5]benzothiazepine derivatives. Synthesis, structure–activity relationships, and molecular modeling studies. *J. Med. Chem.* **1994**, *37*, 1427–1438.

(28) Butini, S.; Brindisi, M.; Cosconati, S.; Marinelli, L.; Borrelli, G.; Coccone, S. S.; Ramunno, A.; Campiani, G.; Novellino, E.; Zanolli, S.; Samuele, A.; Giorgi, G.; Bergamini, A.; Di Mattia, M.; Lalli, S.; Galletti, B.; Gemma, S.; Maga, G. Specific targeting of highly conserved residues in the HIV-1 reverse transcriptase primer grip region. 2. Stereoselective interaction to overcome the effects of drug resistant mutations. *J. Med. Chem.* **2009**, *52*, 1224–1228.

(29) Campiani, G.; Morelli, E.; Fabbrini, M.; Nacci, V.; Greco, G.; Novellino, E.; Ramunno, A.; Maga, G.; Spadari, S.; Caliendo, G.; Bergamini, A.; Faggioli, E.; Uccella, I.; Bolacchi, F.; Marini, S.; Coletta, M.; Nacca, A.; Caccia, S. Pyrrolobenzoxazepinone derivatives as non-nucleoside HIV-1 RT inhibitors: further structure–activity relationship studies and identification of more potent broad-spectrum HIV-1 RT inhibitors with antiviral activity. *J. Med. Chem.* **1999**, *42*, 4462–4470.

(30) Campiani, G.; Nacci, V.; Fiorini, I.; De Filippis, M. P.; Garofalo, A.; Greco, G.; Novellino, E.; Altamura, S.; Di Renzo, L. Pyrrolobenzothiazepinones and pyrrolobenzoxazepinones: novel and specific non-nucleoside HIV-1 reverse transcriptase inhibitors with antiviral activity. *J. Med. Chem.* **1996**, *39*, 2672–2680.

(31) Maga, G.; Gemma, S.; Fattorusso, C.; Locatelli, G. A.; Butini, S.; Persico, M.; Kukreja, G.; Romano, M. P.; Chiasserini, L.; Savini, L.; Novellino, E.; Nacci, V.; Spadari, S.; Campiani, G. Specific targeting of hepatitis C virus NS3 RNA helicase. Discovery of the potent and selective competitive nucleotide-mimicking inhibitor QU663. *Biochemistry* **2005**, *44*, 9637–9644.

(32) Campiani, G.; Fiorini, I.; De Filippis, M. P.; Ciani, S. M.; Garofalo, A.; Nacci, V.; Giorgi, G.; Segal, B.; Botta, M.; Chiarini, A.; Budriesi, R.; Bruni, G.; Romeo, M. R.; Manzoni, C.; Mennini, T. Cardiovascular characterization of pyrrolo[2,1-*d*][1,5]benzothiazepine derivatives binding selectively to the peripheral-type benzodiazepine receptor (PBR): from dual PBR affinity and calcium antagonist activity to novel and selective calcium entry blockers. *J. Med. Chem.* **1996**, *39*, 2922–2938.

(33) Campiani, G.; Nacci, V.; Fiorini, I.; De Filippis, M. P.; Garofalo, A.; Ciani, S. M.; Greco, G.; Novellino, E.; Williams, D. C.; Zisterer, D. M.; Woods, M. J.; Mihai, C.; Manzoni, C.; Mennini, T. Synthesis, biological activity, and SARs of pyrrolobenzoxazepine derivatives, a new class of specific “peripheral-type” benzodiazepine receptor ligands. *J. Med. Chem.* **1996**, *39*, 3435–3450.

(34) Muchmore, S. W.; Smith, R. A.; Stewart, A. O.; Cowart, M. D.; Gomtsyan, A.; Matulenka, M. A.; Yu, H.; Severin, J. M.; Bhagwat, S. S.; Lee, C. H.; Kowaluk, E. A.; Jarvis, M. F.; Jakob, C. L. Crystal structures of human adenosine kinase inhibitor complexes reveal two distinct binding modes. *J. Med. Chem.* **2006**, *49*, 6726–6731.

(35) Henzler-Wildman, K. A.; Lei, M.; Thai, V.; Kerns, S. J.; Karplus, M.; Kern, D. A hierarchy of timescales in protein dynamics is linked to enzyme catalysis. *Nature* **2007**, *450*, 913–916.

(36) Mondello, C.; Chiesa, M.; Rebuzzini, P.; Zongaro, S.; Verri, A.; Colombo, T.; Giulotto, E.; D’Incalci, M.; Franceschi, C.; Nuzzo, F. Karyotype instability and anchorage-independent growth in telomerase-immortalized fibroblasts from two centenarian individuals. *Biochem. Biophys. Res. Commun.* **2003**, *308*, 914–921.

(37) Miller, R. L.; Adamczyk, D. L.; Miller, W. H.; Koszalka, G. W.; Rideout, J. L.; Beacham, L. M., 3rd; Chao, E. Y.; Haggerty, J. J.; Krenitsky, T. A.; Elion, G. B. Adenosine kinase from rabbit liver. II. Substrate and inhibitor specificity. *J. Biol. Chem.* **1979**, *254*, 2346–2352.

(38) Park, J.; Singh, B.; Gupta, R. S. Inhibition of adenosine kinase by phosphonate and bisphosphonate derivatives. *Mol. Cell. Biochem.* **2006**, *283*, 11–21.

(39) Hashemi, M.; Karami-Tehrani, F.; Ghavami, S.; Maddika, S.; Los, M. Adenosine and deoxyadenosine induces apoptosis in oestrogen receptor-positive and -negative human breast cancer cells via the intrinsic pathway. *Cell Proliferation* **2005**, *38*, 269–285.

(40) Liu, Y.; Zhang, Y. Temperature-controlled selective reduction of arenesulfonyl chlorides promoted by samarium metal in DMF. *Tetrahedron Lett.* **2003**, *44*, 4291–4294.

(41) Wang, C.; Batsanov, A. S.; Bryce, M. R.; Sage, I. An improved synthesis and structural characterisation of 2-(4-acetylthiophenylethynyl)-4-nitro-5-phenylethynylaniline: the molecule showing high negative differential resistance (NDR). *Synthesis* **2003**, *13*, 2089–2095.

(42) Reddy, K. R.; Venkateshwar, M.; Maheswari, C. U.; Kumar, P. S. Mild and efficient oxy-iodination of alkynes and phenols with potassium iodide and *tert*-butyl hydroperoxide. *Tetrahedron Lett.* **2010**, *51*, 2170–2173.

(43) Hashima, H.; Hayashi, M.; Kamano, Y.; Sato, N. Synthesis and biological activities of the marine bryozoan alkaloids convolutamines A, C and F, and lutamides A and C. *Bioorg. Med. Chem.* **2000**, *8*, 1757–1766.

(44) Shen, Y.; Sheng, R.; Zhang, J.; He, Q.; Yang, B.; Hu, Y. 2-Phenoxy-indan-1-one derivatives as acetylcholinesterase inhibitors: a study on the importance of modifications at the side chain on the activity. *Bioorg. Med. Chem.* **2008**, *16*, 7646–7653.

(45) Manikowski, A.; Verri, A.; Lossani, A.; Gebhardt, B. M.; Gambino, J.; Focher, F.; Spadari, S.; Wright, G. E. Inhibition of herpes simplex virus thymidine kinases by 2-phenylamino-6-oxopurines and related compounds: structure–activity relationships and antiherpetic activity in vivo. *J. Med. Chem.* **2005**, *48*, 3919–3929.

(46) La Motta, C.; Sartini, S.; Mugnaini, L.; Salerno, S.; Simorini, F.; Taliani, S.; Marini, A. M.; Da Settimo, F.; Lavecchia, A.; Novellino, E.; Antoniolì, L.; Fornai, M.; Blandizzi, C.; Del Tacca, M. Exploiting the pyrazolo[3,4-*d*]pyrimidin-4-one ring system as a useful template to obtain potent adenosine deaminase inhibitors. *J. Med. Chem.* **2009**, *52*, 1681–1692.

(47) Huey, R.; Morris, G. M.; Olson, A. J.; Goodsell, D. S. A semiempirical free energy force field with charge-based desolvation. *J. Comput. Chem.* **2007**, *28*, 1145–1152.

(48) Lavecchia, A.; Cosconati, S.; Limongelli, V.; Novellino, E. Modeling of Cdc25B dual specificity protein phosphatase inhibitors: docking of ligands and enzymatic inhibition mechanism. *ChemMedChem* **2006**, *1*, 540–550.

(49) Limongelli, V.; Marinelli, L.; Cosconati, S.; Braun, H. A.; Schmidt, B.; Novellino, E. Ensemble-docking approach on BACE-1: pharmacophore perception and guidelines for drug design. *ChemMedChem* **2007**, *2*, 667–678.

(50) Simoni, D.; Gebbia, N.; Invidiata, F. P.; Eleopra, M.; Marchetti, P.; Rondanin, R.; Baruchello, R.; Provera, S.; Marchioro, C.; Tolomeo, M.; Marinelli, L.; Limongelli, V.; Novellino, E.; Kwaasi, A.; Dunford, J.; Buccheri, S.; Caccamo, N.; Dieli, F. Design, synthesis, and biological evaluation of novel aminobisphosphonates possessing an in vivo anti-tumor activity through a gammadelta-T lymphocytes-mediated activation mechanism. *J. Med. Chem.* **2008**, *51*, 6800–6807.

(51) *Glide*, version 5.5; Schrodinger, LLC: New York, 2009.